

- ・ **好中球減少症**：好中球減少は3～4週後でも起こることがある。患者状態が良好で発熱がなければ特に処置は不要であるが、投与日における白血球や好中球の確認は毎回行うほうが望ましい。day1においても回復遅延がみられることはしばしばであるためである。
- ・ **倦怠感・無力症**：特に対処はないが、病状の進行による症状ではないかと患者が不安に陥らないよう説明は必要であろう。病状が許せば減量や休薬も選択肢になるとと思われる。
- ・ **便秘**：ビンORELビン（ビノレルビン）は便秘の起こる薬剤であるから、当初より緩下剤などの処方 considering。
- ・ **血管外漏出**：ビンORELビン投与に際しては、血管外漏出に十分注意して、よい静脈路を確保することが重要である。化学療法歴が長期にわたる場合は、よい静脈路の確保も困難である場合がしばしばあるため、必要であればCVポート留置も考慮すべきである。血管外漏出が疑われたときは、vesicant drugの血管外漏出の一般的な処置と同様、直ちにビンORELビンの投与を中止し、漏出が疑われる範囲よりも広範囲に生食・ステロイドの注入を行う。また、ビンORELビンが漏出したときは局所を温めた方がよい。

## ■ まとめ

- ビノレルビンは比較的有害事象が軽度で奏効率の高い薬剤である。
- 特にトラスツズマブとの併用療法で高い奏効率を示し、HER2陽性進行再発乳癌に対して、トラスツズマブ+タキサンと同程度の有効性を示すデータがある。
- ビノレルビンは単剤あるいは併用（特にカペシタビンとの併用やトラスツズマブとの併用）で有効な薬剤である。
- 主な有害事象は骨髄毒性、倦怠感・無力症、便秘などである。
- vesicant drugであるため、血管外漏出には注意が必要である。

（菰池佳史）

## ■ 参考文献

- 1) Burstein H, et al : Trastuzumab and Vinorelbine as First-Line Therapy for HER2-Overexpressing Metastatic Breast Cancer: Multicenter Phase II Trial With Clinical Outcomes, Analysis of Serum Tumor Markers as Predictive Factors, and Cardiac Surveillance Algorithm. *J Clin Oncol*, 21: 2889-2895, 2003.
- 2) Burstein H, et al : Trastuzumab Plus Vinorelbine or Taxane Chemotherapy for HER2-overexpressing Metastatic Breast Cancer: The Trastuzumab and Vinorelbine or Taxane Study. *Cancer*, 110: 965-972, 2007.
- 3) Andersson M, et al : Phase III Randomized Study Comparing Docetaxel Plus Trastuzumab With Vinorelbine Plus Trastuzumab As First-Line Therapy of Metastatic or Locally Advanced Human Epidermal Growth Factor Receptor 2-Positive Breast Cancer: The HERNATA Study. *J Clin Oncol*, 29: 264-271, 2010.
- 4) Zhang J, et al : Vinorelbine and capecitabine in anthracycline- and/or taxanepretreated metastatic breast cancer: sequential or combinational?. *Cancer Chemother Pharmacol*, 71: 103-113, 2013.
- 5) Tan WW, et al : Phase II Interventional Study (N0337) of Capecitabine in Combination With Vinorelbine and Trastuzumab for First- or Second-Line Treatment of HER2-Positive Metastatic Breast Cancer: A North Central Cancer Treatment Group Trial. *Clin Breast Cancer*, 12, 81-86, 2012.
- 6) Pallis AG, et al : A multicenter randomized phase III trial of vinorelbine/gemcitabine doublet versus capecitabine monotherapy in anthracycline- and taxane-pretreated women with metastatic breast cancer. *Ann Oncol*, 23 (5): 1164-1169, 2012
- 7) Stemmler HJ, et al : Randomised phase II trial of gemcitabine plus vinorelbine vs gemcitabine plus cisplatin vs gemcitabine plus capecitabine in patients with pretreated metastatic breast cancer. *Br J Cancer*, 29; 104 (7): 1071-1078, 2011
- 8) Lin NU, et al : A phase II study of bevacizumab in combination with vinorelbine and trastuzumab in HER2-positive metastatic breast cancer. *Breast Cancer Res Treat*. 139 (2): 403-410, 2013

## 術後内分泌療法— 7

## 効果予測因子

- 術後内分泌療法は、エストロゲン受容体 (estrogen receptor ; ER) 陽性早期乳癌の術後薬物療法の第1選択として行われる。
- 内分泌療法はERを標的とする治療であり、乳癌組織におけるERの発現が内分泌療法の効果予測因子であり大前提である。
- 一方、各内分泌療法剤 (タモキシフェンやアロマターゼ阻害薬など) の効果は、ERの発現のような癌細胞の生物学的特性だけではなく、宿主要因も関与する。
- 術後内分泌療法の効果予測因子としては、内分泌療法の効果予測因子と各内分泌療法剤特有の効果予測因子が存在する。
- 術後内分泌療法の効果の指標は「予後」となるため、これまで報告されている効果予測因子のほとんどはER陽性乳癌の予後予測因子となっている。
- 本項では、ER陽性乳癌の予後予測因子、内分泌療法の効果予測因子について因子ごとに概説し、各内分泌療法剤特有の効果予測因子についての現在の知見も述べる。
- 表1に、ER陽性HER2陰性乳癌の術後薬物療法に際して考慮する因子 (2009年St.Gallen<sup>1)</sup>) を示した。

表1 ER陽性HER2陰性乳癌の術後薬物療法に際して考慮する因子

	内分泌療法感受性		
	化学・内分泌療法の 相対的適応	決定に役立たない因子	内分泌療法単独の 相対的適応
ER・PgR陽性細胞率	低い	—	高い
増殖能 (Ki67 labeling index)	高い	中間	低い
Grade	3	2	1
多遺伝子発現解析	高リスク	中リスク	低リスク
腫瘍浸潤径 (pT)	>5cm	2.1～5cm	≤2cm
腋窩リンパ節転移	≥4個	1～3個	なし
脈管浸潤 (PVI)	広範なPVIがある	—	広範なPVIがない
患者の嗜好	すべての可能な治療	—	副作用は避けたい

スペクトラムは連続的、かつ、環境 (治療や宿主の要因など) によって変化する可能性がある。腫瘍浸潤径、腋窩リンパ節転移個数、脈管浸潤はER陽性HER2陰性乳癌の再発リスク因子。

(文献1)より改変)

## ■ 生物学的因子

### 1 ホルモン受容体：ER, プロゲステロン受容体 (progesterone receptor ; PgR)

- 乳癌組織におけるホルモン受容体 (ER, PgR) の発現は、IHC法により評価する。
- 2010年のASCO/CAP (米国臨床腫瘍学会/米国病理医会) のガイドラインでは、癌細胞の核に少なくとも1%の染色陽性細胞がある場合ER/PgR陽性と判定することが推奨されている<sup>2)</sup>。また、ER陰性乳癌への内分泌療法の有効性は認めないことが明記されている。
- ER/PgRの発現量 (陽性細胞率) は症例によりさまざまな分布を示し、0%から100%まで連続的に存在する。
- ER陽性乳癌術後のタモキシフェンの予後改善効果を示すEBCTCGのメタアナリシスによると、ER陽性乳癌においてタモキシフェン5年投与はER, PgRの発現量にかかわらず再発抑制効果を示した<sup>3)</sup>。
- さらに、タモキシフェンの5年投与により、コントロール (内服なし) に比べて再発率が4割、死亡率が3割低下した<sup>3)</sup>。
- **エストロゲン受容体 (ER)**
  - ・ Allredらは術後内分泌療法を行った症例の予後を解析し、ERの発現量が高いほど予後良好であり、Allred Score 3以上 (陽性細胞率1%以上) で術後内分泌療法の予後改善効果があることを報告した<sup>4)</sup>。
  - ・ 閉経後の術後内分泌療法の臨床試験 (ATAC試験とBIG1-98試験) において、アロマターゼ阻害薬群、タモキシフェン群ともにERの陽性細胞率が高いほど予後良好であり<sup>5)</sup>、ERの陽性細胞率1%をカットオフとした場合、陽性例で有意に予後良好で、内分泌療法の効果が期待できる<sup>6)</sup>と報告された。
  - ・ 現在、乳癌組織のERの発現量は術後内分泌療法の奏効性や予後に関与すると考えられている。
- **プロゲステロン受容体 (PgR)**
  - ・ 閉経後の術後内分泌療法の臨床試験 (ATAC試験とBIG1-98試験) において、アロマターゼ阻害薬群、タモキシフェン群ともにPgRの陽性細胞率が高いほど予後良好であり<sup>5)</sup>、陽性細胞率1%をカットオフとした場合、陽性例で有意に予後良好であった<sup>6)</sup>。また、PgR発現量にかかわらずレトロゾール群がタモキシフェン群より予後良好であった<sup>6)</sup>。
  - ・ 現在、乳癌組織のPgRの発現量は、閉経後ER陽性乳癌の予後因子と考えられている。

### 2 human epidermal growth factor receptor 2 (HER2)

- 閉経後の術後内分泌療法の臨床試験 (ATAC試験とBIG1-98試験) において、アロマターゼ阻害薬群、タモキシフェン群ともにHER2陰性例が予後良好であり、HER2発現にかかわらずアロマターゼ阻害薬群が予後良好であった<sup>5,7)</sup>。

### 3 Ki67

- Ki67はG0期以外のすべての細胞周期において核内に発現しているタンパクで、増殖の指標である。
- 通常、IHC法にて陽性細胞率（labeling index）を評価する。
- Ki67 labeling indexは、グレード（組織学的グレードまたは核グレード）の、特に核分裂像（mitotic counts）と相関する。
- 閉経後の術後内分泌療法の臨床試験（BIG1-98試験）において、Ki67低発現群はKi67高発現群に比べて有意に予後良好であり、Ki67高発現群においてはレトロゾール群がタモキシフェン群に比べて有意に予後良好であった<sup>8)</sup>。
- 閉経後の術後内分泌療法の臨床試験（ATAC試験）において、IHC4 Score（ER, PgR, HER2, Ki67）はER陽性乳癌の予後予測因子であった<sup>9)</sup>。
- 2007年、2008年のメタアナリシスではKi67は乳癌の予後因子であることが示されている<sup>10, 11)</sup>。
- リンパ節転移陽性乳癌の術後化学療法の臨床試験（BCIRG 001試験とPACS 01試験）の後ろ向き研究において、ER陽性乳癌のうちKi67高発現群は、アンストラサイクリン系薬剤にタキサン系薬剤を追加することにより、アンストラサイクリン系薬剤のみの群より予後が改善した<sup>12, 13)</sup>。
- 現在、乳癌組織のKi67高発現は、ER陽性乳癌における早期（5年以内）再発の予後予測因子であり、ER陽性Ki67高発現乳癌においては化学療法（タキサン系薬）を追加することにより予後改善が期待できる指標と考えられている。
- Ki67の評価方法、カットオフなどについては現在、いまだ標準化されていない。

### 4 多遺伝子アッセイ

- IMPAKT Working Groupからの報告では、現在開発されている6つの多遺伝子アッセイ（Oncotype Dx<sup>®</sup>, MammaPrint<sup>®</sup>, Genomic Grade Index, PAM50, Breast Cancer Index, EndoPredict）を用いた場合に予後が改善するかは、現時点では不明確であると結論している<sup>14)</sup>。
- **Oncotype Dx<sup>®</sup> (RS)**
  - 乳癌組織（パラフィンブロック）を用いて21遺伝子のmRNA発現を評価し、再発スコア（21-gene recurrence score; RS）を算出する<sup>15)</sup>。ER陽性乳癌を対象としたレトロスペクティブ研究で高リスクと判定された場合は、タモキシフェンに化学療法（CMF療法）を追加することにより予後の改善が得られた。

- ・これまでのレトロスペクティブ研究により、現在、対象はER陽性・Stage I/IIかつリンパ節転移陰性症例と、閉経後ER陽性・Stage II/IIIかつリンパ節転移陽性 (N1) 症例となっている<sup>16)</sup>。
- ・術後内分泌療法の臨床試験 (ATAC試験) において、RSはER陽性乳癌の予後予測因子であった<sup>17)</sup>。
- ・ER陽性リンパ節転移陰性乳癌で内分泌療法単独の術後薬物療法施行症例 (NSABP B-14試験とATAC試験) において、RSに臨床病理学的因子 (年齢、腫瘍径、Grade) を加えることにより、RS単独よりも中間リスク群に分類される症例を減らすことができた<sup>18)</sup>。
- ・ER陽性乳癌におけるOncotype DX<sup>®</sup>を用いた前向き試験として、リンパ節転移陰性症例を対象としたTAILORx試験、リンパ節転移陽性 (1～3個) 症例を対象としたRxPONDER (SWOG S1007) 試験が進行中である。

#### ● MammaPrint<sup>®</sup> (70-gene signature)

- ・凍結乳癌組織を用いて70遺伝子のmRNA発現を評価する。ER、HER2状況は問わず、再発の有無をもとに25,000遺伝子のなかから抽出された70遺伝子による予後予測ツールである<sup>19)</sup>。
- ・これまでの後ろ向き研究により、現在、対象はStage I/II、リンパ節転移陰性あるいは陽性 (1～3個) となっている<sup>16)</sup>。
- ・最近の観察研究 (RASTER 研究) では427人のリンパ節転移陰性症例が登録され、Adjuvant! OnlineにMammaPrint<sup>®</sup>を加えることで5年遠隔無再発リスク評価が改善したことが報告された<sup>20)</sup>。
- ・現在、MammaPrint<sup>®</sup>を用いたランダム化比較試験であるMicroarray In Node-negative Disease may Avoid Chemotherapy Trial (MINDACT) が、リンパ節転移陰性の早期乳癌症例 6,000例を対象に進行中である。

## ■ 宿主要因

### 1 タモキシフェンの効果とCYP2D6遺伝子多型

- CYP2D6 (チトクロムP450) はタモキシフェンを活性体のエンドキシフェンに変換する酵素である。
- CYP2D6阻害薬のパロキセチン (抗うつ薬) をタモキシフェンと併用すると、血漿中のエンドキシフェン濃度が低くなりタモキシフェンの効果が期待できない可能性がある。
- CYP2D6 \*4のホモタイプ (\*4/\*4) は血漿中のエンドキシフェン濃度が低いことが報告され、このタイプの患者 (欧米人の5～10%) はタモキシフェンの効果が期待できない可能性がある。
- 術後タモキシフェン5年投与を行った欧米の臨床試験の患者において、CYP2D6 \*4のホモタイプは予後不良であった<sup>21)</sup>。
- 閉経後の術後内分泌療法の臨床試験 (ATAC試験とBIG1-98試験) における最近の報告では、いずれの臨床試験においてもタモキシフェン群においてCYP2D6遺伝子多型と予後に相関はみられなかった<sup>22, 23)</sup>。

- アジア人のCYP2D6\*4ホモタイプは1%未満と報告されているが,\*10のホモタイプ(CYP2D6の活性がやや低下する)は15~20%に存在する。
- 日本人におけるCYP2D6遺伝子多型の検討では、術後タモキシフェン投与例においてCYP2D6\*10遺伝子多型による予後の差はないと報告されている<sup>24,25)</sup>。

## 2 内分泌療法関連副作用と予後

- 閉経後の術後内分泌療法の臨床試験(ATAC試験とTEAM試験)において、内分泌療法関連副作用(関節症状、ホットフラッシュ、寝汗など)の出現と再発率をみたところ、いずれの臨床試験においても症状があった群はなかった群に比べて再発率が低かった<sup>26,27)</sup>。
- アロマトラーゼ阻害薬に伴う筋骨格系の副作用(関節痛、筋肉痛など)に関連する遺伝子多型を同定する研究が行われ、一塩基多型(SNPs; rs11849538)が同定された<sup>28)</sup>。
- 同定したSNPs(rs11849538)はTCL1A遺伝子のプロモーター領域に存在し、ERの結合部位を生じる。アロマトラーゼ阻害薬による筋骨格系の副作用が強い女性には、バリエーションタイプをもつ人が多かった<sup>28)</sup>。

## 3 body mass index (BMI) と予後

- 閉経後の欧米人女性において、血清エストロゲン濃度はBMIと正相関する。
- 閉経後の術後内分泌療法の臨床試験(ATAC試験)において、肥満(BMI>35)女性はBMI<23の女性に比べて再発率が高かった。また、BMI>30の女性ではタモキシフェン群とアナストロゾール群で再発率に差を認めなかった<sup>29)</sup>。
- 閉経前の術後内分泌療法の臨床試験(ABCSG-12試験;ゴセレリン/タモキシフェンvs.ゴセレリン/アナストロゾール)において、BMI≥25以上の人はアナストロゾール群がタモキシフェン群より予後不良であった<sup>30)</sup>。

## まとめ

- ER陽性乳癌の予後はこの30年間で明らかに改善した<sup>31)</sup>。これは再発予防目的として行う術後内分泌療法を中心とした薬物療法の進歩によると考えられている。
- しかしながら、特に腋窩リンパ節転移陽性症例は術後5年以降の再発リスクも高く、いかにこのような晩期再発症例の予後を改善するかが課題の1つである。
- そのために、より長期の内分泌療法や適切な内分泌療法薬の選択のほか、現在行っている内分泌療法や化学療法とは作用機序の異なる新たな薬物療法の開発が進められている。

(山下啓子)

## ■ 参考文献

- 1) Goldhirsch A, et al : Thresholds for therapies : highlights of the St Gallen International Expert Consensus on the primary therapy of early breast cancer 2009. *Ann Oncol*, 20 (8): 1319-1329, 2009.
- 2) Hammond ME, et al : American Society of Clinical Oncology/College of American Pathologists guideline recommendations for immunohistochemical testing of estrogen and progesterone receptors in breast cancer. *J Clin Oncol*, 28 (16): 2784-2795, 2010.
- 3) Davies C, et al : Relevance of breast cancer hormone receptors and other factors to the efficacy of adjuvant tamoxifen: patient-level meta-analysis of randomised trials. *Lancet*, 378 (9793): 771-784, 2011.
- 4) Harvey JM, et al : Estrogen receptor status by immunohistochemistry is superior to the ligand-binding assay for predicting response to adjuvant endocrine therapy in breast cancer. *J Clin Oncol*, 17 (5): 1474-1481, 1999.
- 5) Dowsett M, et al : Relationship between quantitative estrogen and progesterone receptor expression and human epidermal growth factor receptor 2 (HER-2) status with recurrence in the Arimidex, Tamoxifen, Alone or in Combination trial. *J Clin Oncol*, 26 (9): 1059-1065, 2008.
- 6) Viale G, et al : Prognostic and predictive value of centrally reviewed expression of estrogen and progesterone receptors in a randomized trial comparing letrozole and tamoxifen adjuvant therapy for postmenopausal early breast cancer: BIG 1-98. *J Clin Oncol*, 25 (25): 3846-3852, 2007.
- 7) Rasmussen BB, et al : Adjuvant letrozole versus tamoxifen according to centrally-assessed ERBB2 status for postmenopausal women with endocrine-responsive early breast cancer: supplementary results from the BIG 1-98 randomised trial. *Lancet Oncol*, 9 (1): 23-28, 2008.
- 8) Viale G, et al : Prognostic and predictive value of centrally reviewed Ki-67 labeling index in postmenopausal women with endocrine-responsive breast cancer: results from Breast International Group Trial 1-98 comparing adjuvant tamoxifen with letrozole. *J Clin Oncol*, 26 (34): 5569-5575, 2008.
- 9) Cuzick J, et al : Prognostic value of a combined estrogen receptor, progesterone receptor, Ki-67, and human epidermal growth factor receptor 2 immunohistochemical score and comparison with the Genomic Health recurrence score in early breast cancer. *J Clin Oncol*, 29 (32): 4273-4278, 2011.
- 10) de Azambuja E, et al : Ki-67 as prognostic marker in early breast cancer: a meta-analysis of published studies involving 12,155 patients. *Br J Cancer*, 96 (10): 1504-1513, 2007.
- 11) Stuart-Harris R, et al : Proliferation markers and survival in early breast cancer: a systematic review and meta-analysis of 85 studies in 32,825 patients. *Breast*, 17 (4): 323-334, 2008.
- 12) Hugh J, et al : Breast cancer subtypes and response to docetaxel in node-positive breast cancer: use of an immunohistochemical definition in the BCIRG 001 trial. *J Clin Oncol*, 27 (8): 1168-1176, 2009.
- 13) Penault-Llorca F, et al : Ki67 expression and docetaxel efficacy in patients with estrogen receptor-positive breast cancer. *J Clin Oncol*, 27 (17): 2809-2815, 2009.
- 14) Azim HA, Jr, et al : Utility of prognostic genomic tests in breast cancer practice: The IMPAKT 2012 Working Group Consensus Statement. *Ann Oncol*, 24 (3): 647-654, 2013.
- 15) Paik S, et al : A multigene assay to predict recurrence of tamoxifen-treated, node-negative breast cancer. *N Engl J Med*, 351 (27): 2817-2826, 2004.
- 16) 日本乳癌学会編 : 科学的根拠に基づく 乳癌診療ガイドライン ①治療編 2011年版. 金原出版, 東京, 2011.
- 17) Dowsett M, et al : Prediction of risk of distant recurrence using the 21-gene recurrence score in node-negative and node-positive postmenopausal patients with breast cancer treated with anastrozole or tamoxifen: a TransATAC study. *J Clin Oncol*, 28 (11): 1829-1834, 2010.
- 18) Tang G, et al : Risk of recurrence and chemotherapy benefit for patients with node-negative, estrogen receptor-positive breast cancer: recurrence score alone and integrated with pathologic and clinical factors. *J Clin Oncol*, 29 (33): 4365-4372, 2011.
- 19) van de Vijver MJ, et al : A gene-expression signature as a predictor of survival in breast cancer. *N Engl J Med*, 347 (25): 1999-2009, 2002.
- 20) Drukker CA, et al : A prospective evaluation of a breast cancer prognosis signature in the observational RASTER study. *Int J Cancer*, 2013.
- 21) Goetz MP, et al : Pharmacogenetics of tamoxifen biotransformation is associated with clinical outcomes of efficacy and hot flashes. *J Clin Oncol*, 23 (36): 9312-9318, 2005.
- 22) Regan MM, et al : CYP2D6 genotype and tamoxifen response in postmenopausal women with endocrine-responsive breast cancer: the breast international group 1-98 trial. *J Natl Cancer Inst*, 104 (6): 441-451, 2012.
- 23) Rae JM, et al : CYP2D6 and UGT2B7 genotype and risk of recurrence in tamoxifen-treated breast cancer patients. *J Natl Cancer Inst*, 104 (6): 452-460, 2012.
- 24) Okishiro M, et al : Genetic polymorphisms of CYP2D6 10 and CYP2C19 2, 3 are not associated with prognosis, endometrial thickness, or bone mineral density in Japanese breast cancer patients treated with adjuvant tamoxifen. *Cancer*, 115 (5): 952-961, 2009.
- 25) Toyama T, et al : No association between CYP2D6\*10 genotype and survival of node-negative Japanese breast cancer patients receiving adjuvant tamoxifen treatment. *Jpn J Clin Oncol*, 39 (10): 651-656, 2009.
- 26) Cuzick J, et al : Treatment-emergent endocrine symptoms and the risk of breast cancer recurrence: a retrospective analysis of the ATAC trial. *Lancet Oncol*, 9 (12): 1143-1148, 2008.
- 27) Fontein DB, et al : Specific Adverse Events Predict Survival Benefit in Patients Treated With Tamoxifen or Aromatase Inhibitors: An International Tamoxifen Exemestane Adjuvant Multinational Trial Analysis. *J Clin Oncol*, 2013.
- 28) Ingle JN, et al : Genome-wide associations and functional genomic studies of musculoskeletal adverse events in women receiving aromatase inhibitors. *J Clin Oncol*, 28 (31): 4674-4682, 2010.
- 29) Sestak I, et al : Aromatase inhibitor-induced carpal tunnel syndrome: results from the ATAC trial. *J Clin Oncol*, 27 (30): 4961-4965, 2009.
- 30) Pfeiler G, et al : Impact of body mass index on the efficacy of endocrine therapy in premenopausal patients with breast cancer: an analysis of the prospective ABCSG-12 trial. *J Clin Oncol*, 29 (19): 2653-2659, 2011.
- 31) Yamashita H, et al : Estrogen receptor-positive breast cancer in Japanese women: trends in incidence, characteristics, and prognosis. *Ann Oncol*, 22 (6): 1318-1325, 2011.

## Case Report

## First clinical trial of cancer vaccine therapy with artificially synthesized helper/killer-hybrid epitope long peptide of MAGE-A4 cancer antigen

Norihiro Takahashi,<sup>1,6</sup> Takayuki Ohkuri,<sup>2,6</sup> Shigenori Homma,<sup>1</sup> Junya Ohtake,<sup>2</sup> Daiko Wakita,<sup>2</sup> Yuji Togashi,<sup>3</sup> Hidemitsu Kitamura,<sup>2</sup> Satoru Todo<sup>1,4</sup> and Takashi Nishimura<sup>2,5</sup><sup>1</sup>First Department of Surgery, Hokkaido University School of Medicine, Sapporo; <sup>2</sup>Division of Immunoregulation, Section of Disease Control, Institute for Genetic Medicine, Hokkaido University, Sapporo; <sup>3</sup>Bioluminance Co, Ltd, Sapporo; <sup>4</sup>Department of Organ Transplantation, Hokkaido University Graduate School of Medicine, Sapporo, Japan

(Received August 31, 2011/Revised September 12, 2011/Accepted September 15, 2011)

A patient with pulmonary metastasis of colon cancer was treated with artificially synthesized helper/killer-hybrid epitope long peptide (H/K-HELP) of MAGE-A4 cancer antigen. The patient was vaccinated with MAGE-A4-H/K-HELP combined with OK432 and Montanide ISA-51. There were no severe side-effects except for a skin reaction at the injection site. MAGE-A4-H/K-HELP induced MAGE-A4-specific Th1 and Tc1 immune responses and the production of MAGE-A4-specific complement-fixing IgG antibodies. Tumor growth and carcinoembryonic antigen tumor marker were significantly decreased in the final diagnosis. This is the first report that artificially synthesized MAGE-A4-H/K-HELP induces Th1-dependent cellular and humoral immune responses in a human cancer patient. (*Cancer Sci* 2012; 103: 150–153)

## Case report

First clinical findings in one patient treated with an artificially synthesized MAGE-A4-helper/killer-hybrid epitope long peptide (H/K-HELP) cancer vaccine.

A 62-year-old Japanese man had a history of pulmonary metastasis and resected colon cancer without active infections (human immunodeficiency virus [HIV], hepatitis B virus [HBV] and hepatitis C virus [HCV]), severe heart diseases (New York Heart Association class 3 or 4) and autoimmune diseases (scleroderma, Sjogren's syndrome, idiopathic thrombocytopenic purpura, multiple sclerosis and rheumatoid arthritis). The patient was enrolled in this trial and confirmed MAGE-A4 antigen expression and human leukocyte antigen (HLA)-phenotypes (HLA-A\*310102, A\*330301, and DRB1\*150101).

The pulmonary metastatic colon cancer of the patient was shown to express MAGE-A4 cancer antigen by both immunohistological analysis and real-time PCR (Fig. 1a–e). MAGE-A4-H/K-HELP was artificially synthesized by conjugating MAGE-A4<sub>278–299</sub> helper epitope with MAGE-A4<sub>143–154</sub> killer epitope by a glycine linker (Fig. 1f). In a phase I study, the enrolled patients were treated with subcutaneous injection of MAGE-A4-H/K-HELP (1 or 10 mg) combined with OK432 and Montanide ISA-51 four times at 2-week intervals (Fig. 1g). In the present case, the patient was first treated with 1 mg MAGE-A4-H/K-HELP four times at 2-week intervals and thereafter treated with 10 mg dose-escalated MAGE-A4-H/K-HELP six times. Physical and hematological examinations were monitored before and after vaccination with MAGE-A4 H/K-HELP. As a result, it was confirmed that there were no severe side-effects, although a skin reaction

occurred at the injection site (Grade 2 reaction, Common Terminology Criteria for Adverse Events [CTCAE] v4.0 criteria). The isolated CD4<sup>+</sup> T cells from the patient's PBMC did not produce significant levels of interferon (IFN)- $\gamma$  by stimulation with H/K-HELP in the presence of antigen presenting cells (APC) before vaccination. However, the levels of IFN- $\gamma$  production by CD4<sup>+</sup> T cells greatly increased in the patient after vaccination with 1 mg MAGE-A4-H/K-HELP (Fig. 2a), and the levels of Th1 response increased approximately 10 times after vaccination with 10 mg MAGE-A4-H/K-HELP (data not shown). The numbers of CD8<sup>+</sup> Tc1 cells detected by IFN- $\gamma$ -enzyme-linked immunosorbent spot (ELISPOT) assay also increased in the patient's PBMC after 1 mg MAGE-A4-H/K-HELP vaccination (Fig. 2b), and the increased Tc1 response was also observed after 10 mg vaccination (data not shown). We determined that the epitope recognized by CD4<sup>+</sup> T cells was exactly our identified helper epitope (MAGE-A4<sub>278–299</sub>) in H/K-HELP, while the CD8<sup>+</sup> T cells recognized an unknown new killer epitope in a part of the helper epitope sequence of H/K-HELP (data not shown). Thus, MAGE-A4-H/K-HELP induced both Th1 and Tc1 responses in the patient irrespective of the patient expressing HLA DR1501 bound to MAGE-A4<sub>278–299</sub> helper epitope but not HLA A24 bound to MAGE-A4<sub>143–154</sub> killer epitope in MAGE-A4-H/K-HELP. Moreover, our vaccine protocol with MAGE-A4-H/K-HELP mainly induced MAGE-A4-peptide-specific IgG3 antibody (Ab) and slightly induced IgG1 Ab, both of which are Th1-dependent complement-fixing Ab (Fig. 2c,d). The levels of MAGE-A4-specific IgM also slightly but significantly increased at an early stage of the 1 mg vaccination, but the levels did not change after the 10 mg vaccination. In contrast to IgM, the levels of MAGE-A4-peptide-specific IgG3 and IgG1 Ab greatly increased after the 10 mg vaccination (Fig. 2d). However, no increase in IgG2 and IgG4 was observed after vaccination with H/K-HELP. We demonstrated that MAGE-A4-specific IgG Ab recognized MAGE-A4<sub>143–154</sub> killer epitope in H/K-HELP (data not shown). Thus, it was demonstrated that the MAGE-A4<sub>278–299</sub> helper epitope exactly

<sup>5</sup>To whom correspondence should be addressed.

E-mail: tak24@igm.hokudai.ac.jp

<sup>6</sup>These two authors contributed equally to this work.This study was approved by the Institutional Review Boards of Hokkaido University School of Medicine and Institute for Genetic Medicine, Hokkaido University (Hokkaido, Japan) and registered at UMIN Clinical Trials Registry (<http://www.umin.ac.jp/ctr/index-j.htm>) as UMIN000003489 (Cancer vaccine study with MAGE-A4/Survivin helper peptide). Informed consent for publication was obtained from the patient.



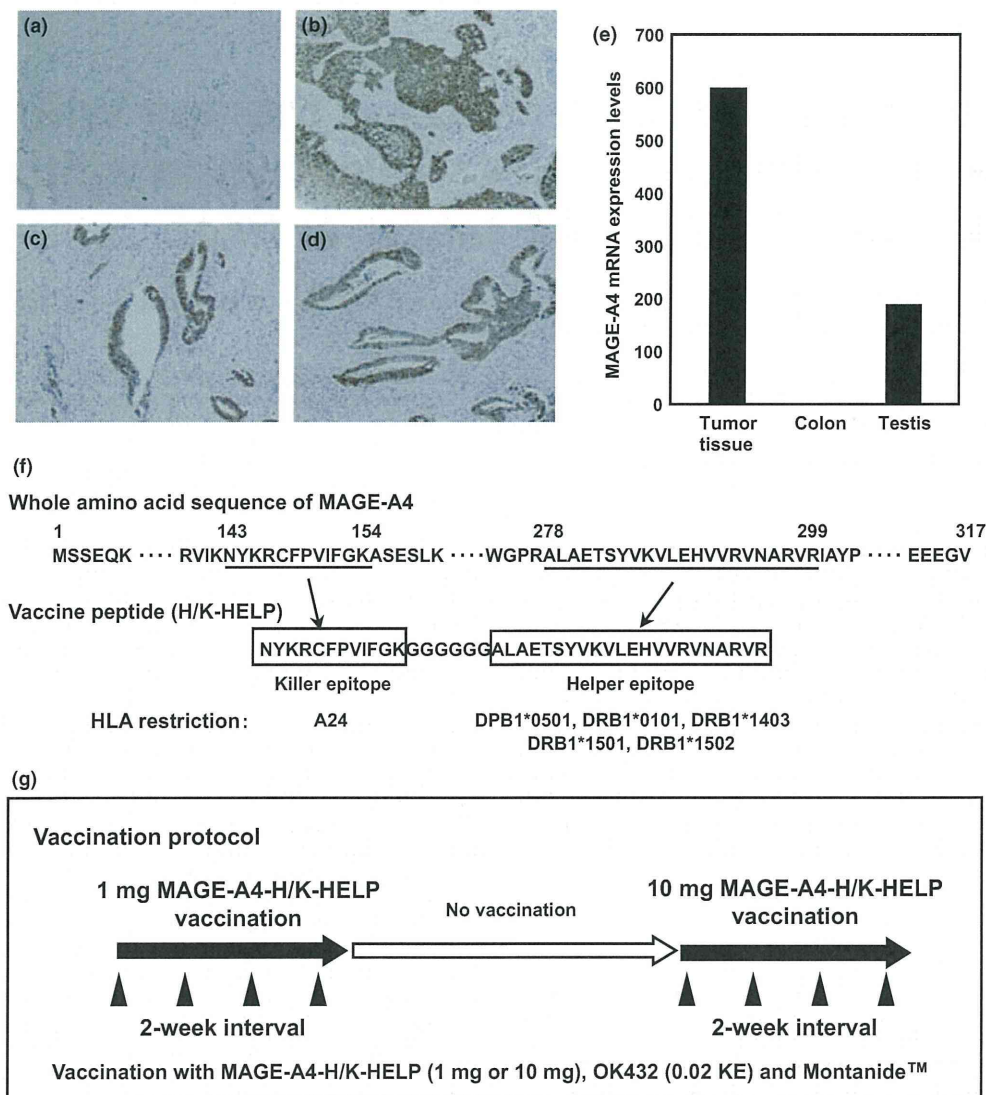


**Fig. 1.** Treatment of a patient with pulmonary metastasis of colon cancer with MAGE-A4-H/K-HELP. Immunohistochemical staining with anti-pan MAGE-A4 mAb (57B) for (a) MAGE-A4<sup>-</sup> bladder cancer (negative control), (b) head and neck cancer (positive control), which revealed similar staining intensity to testis, and (c, d) a tumor tissue sample of the enrolled patient. (e) MAGE-A4 mRNA expression levels were assessed by real-time PCR. Normal colon and testis were used as a negative or positive control, respectively. (f) The amino acid sequence of artificially synthesized MAGE-A4-H/K-HELP used in this trial. MAGE-A4-H/K-HELP was artificially synthesized by conjugating MAGE-A4<sub>278-299</sub> helper epitope (22 amino acid sequence in the right box) with MAGE-A4<sub>143-154</sub> killer epitope (12 amino acid sequence in the left box) by a glycine linker. (g) Vaccination protocol for the patient in a phase I study. The patient was vaccinated with 1 or 10 mg MAGE-A4-H/K-HELP mixed with OK-432 (0.02KE) and Montanide ISA-51 four times at 2-week intervals. H/K-HELP, helper/killer-hybrid epitope long peptide; HLA, human leukocyte antigen.

stimulated CD4<sup>+</sup> T cells and a part of the helper epitope peptide also activated CD8<sup>+</sup> T cells, while the MAGE-A4<sub>143-154</sub> killer epitope triggered the production of MAGE-A4-specific IgG Ab, indicating the long peptide vaccine, H/K-HELP, appeared to be beneficial for inducing both cellular and humoral immune responses in the cancer patient. In parallel with superior immune responses, tumor growth and serum levels of the carcinoembryonic antigen tumor marker were slightly decreased during cancer vaccine therapy with MAGE-A4-H/K-HELP (Fig. 3), and this patient's clinical response was finally judged as stable disease (Response Evaluation Criteria in Solid Tumors [RECIST] v1.1 guidelines<sup>(1)</sup>). This is the first report that cancer vaccine therapy with artificially synthesized MAGE-A4-H/K-HELP induced Th1-dependent cellular and humoral immune responses in a cancer patient. So far, no

severe side-effects were observed in six patients treated with MAGE-A4-H/K-HELP (three patients with 1 mg and three patients with 10 mg, CTCAEv4.0), and significant T-cell responses were demonstrated in 50% of patients (data not shown).

## Discussion

Cancer vaccine therapy using HLA class I-binding 8-9 amino acids short cancer peptide has been performed to induce cancer-specific cytotoxic T lymphocytes (CTL) in cancer patients.<sup>(2,3)</sup> Although cancer vaccine therapy with short peptide induced increased tetramer<sup>+</sup> cancer-specific CTL and long stable disease, the vaccine therapy focused only on CTL activation appears to be suboptimal in conquering cancer.<sup>(4-6)</sup> This might be because

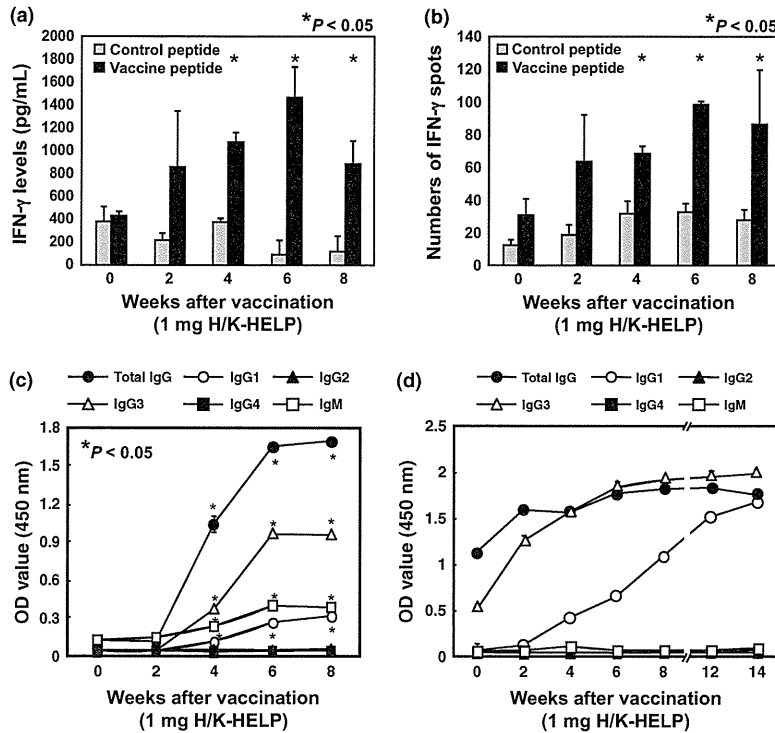


**Fig. 2.** Cellular and humoral immune responses in a patient vaccinated with MAGE-A4-H/K-HELP. (a,b) MAGE-A4-H/K-HELP-specific interferon (IFN)- $\gamma$  production by CD4<sup>+</sup> T cells or CD8<sup>+</sup> T cells was assessed at various weeks after vaccination with MAGE-A4-H/K-HELP (1 mg) by ELISA (a) or enzyme-linked immunosorbent spot (ELISPOT) assay (b), respectively.  $*P < 0.05$ , against control survivin-H/K-HELP peptide. (c) The levels of antibodies (total IgG, ●; IgG1, ○; IgG2, ▲; IgG3, △; IgG4, ■; and IgM, □) against MAGE-A4-H/K-HELP peptide in the patient's serum sample (400-fold diluted) was determined at 2, 4, 6 and 8 weeks after vaccination with 1 mg MAGE-A4-H/K-HELP.  $*P < 0.05$ , against 0 weeks after vaccination. (d) The levels of antibodies (total IgG, ●; IgG1, ○; IgG2, ▲; IgG3, △; IgG4, ■; and IgM, □) against MAGE-A4-H/K-HELP peptide in the patient's serum sample (400-fold diluted) was determined at 2, 4, 6, 8, 10 and 12 weeks after vaccination with 10 mg MAGE-A4-H/K-HELP. H/K-HELP, helper/killer-hybrid epitope long peptide.

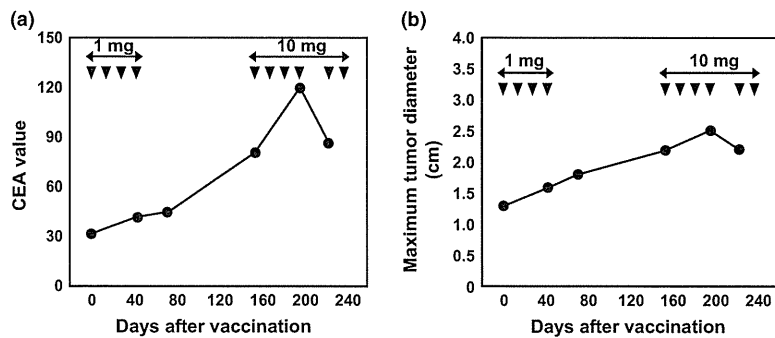


**Fig. 3.** Clinical responses in a colon cancer patient treated with MAGE-A4-H/K-HELP vaccine. (a) The carcinoembryonic antigen (CEA) value in the patient's serum was measured using ELISA on various days after vaccination. (b) Maximum tumor diameter was measured by computer tomography. H/K-HELP, helper/killer-hybrid epitope long peptide.

of the existence of strong immunosuppressive tumor escape mechanisms and the lack of helper T-cell activation.<sup>(7,8)</sup>

Therefore, it is essential to develop an efficient method to overcome immunosuppression to combat cancer. We initially demonstrated the critical role of Th1 and Th2 immunity in the tumor-bearing host and have proposed that the introduction of Th1-dominant immunity is essential for inducing fully activated CTL and immunological memory.<sup>(8-11)</sup> Recently, it has been demonstrated that a mixture of various synthetic long peptides

(SLP) derived from the naturally occurring sequence of human papilloma virus (HPV)-16 oncoproteins was superior to short tumor peptides in terms of inducing a complete or partial response in vulvar intraepithelial neoplasia.<sup>(12)</sup> Zwaveling *et al.*<sup>(13)</sup> also reported that HPV-16-derived 35 amino acid-long peptide eradicated the established HPV-16-expressing mouse tumor. Thus, long peptide vaccine containing both helper and killer epitopes appeared to be a rational strategy to activate Th1-dependent antitumor immunity.<sup>(8)</sup> In contrast to viral-related

cancer antigenic long peptide, p53-long peptide vaccine induced no complete or partial response in a clinical trial of human cancers, although it induced significant T cell responses.<sup>(14,15)</sup> Moreover, the first clinical trial using a synthetic 15 amino acid peptide vaccine containing a naturally occurring combination of helper and killer epitopes of gp100<sub>175-189</sub> exhibited no significant impact for therapeutic efficacy of melanoma.<sup>(16)</sup> Therefore, what kinds of long peptide induce a beneficial therapeutic effect against human cancer still remains unclear.

Here, we prepared an artificially synthesized long peptide, which conjugate MAGE-A4 class I-binding epitope and our defined helper epitope,<sup>(17)</sup> and applied it to a patient with pulmonary metastatic colon cancer. In contrast to short gp100<sub>175-189</sub> peptide including helper and killer epitopes,<sup>(16)</sup> we successfully induced cancer-specific Th1/Tc1 cells and complement-fixing Ab (IgG1 and IgG3)<sup>(18)</sup> by 40 amino acid H/K-HELP. This discrepancy might be because artificially synthesized 40 amino acid-long peptide but not short peptide has a beneficial structure for inducing favorable dendritic cells (DC) presentation and subsequent activation of Th1 and Tc1 cells.

Bijker *et al.*<sup>(19)</sup> reported that SLP of class I-binding long cancer peptide was efficiently processed by professional APC and subsequently exhibited a sustained stimulating activity of DC to induce Th-dependent, tumor-specific CTL.<sup>(19)</sup> We have also

confirmed that ovalbumin (OVA)-H/K-HELP was superior to short peptide in curing mice with OVA-expressing tumor (data not shown). In another clinical trial, we demonstrated that survivin-H/K-HELP induced a complete response in a breast cancer patient (data not shown). Thus, we believe that artificially synthesized H/K-HELP of cancer antigen will become a promising tool to induce Th1-dependent cellular and humoral immunity in cancer patients, as well as SLP derived from natural tumor-associated HPV-16 antigen peptide.<sup>(12)</sup>

## Acknowledgments

The authors thank the patient for consenting to the publication of their clinical details. The authors are also grateful to the clinical research coordinators of Hokkaido University Hospital for their support with the treatment of the patient. This study is part of a "Development of Innovative Cancer Immunotherapy by Helper T cells", sponsored by a Translational Research Promotion Project of the New Energy and Industrial Technology Development Organization (NEDO).

## Disclosure Statement

All authors declare that they have no conflict of interest.

## References

- Eisenhauer EA, Therasse P, Bogaerts J *et al.* New response evaluation criteria in solid tumors: revised RECIST guideline (version 1.1). *Eur J Cancer* 2009; **45**: 228–47.
- van der Bruggen P, Traversari C, Chomez P *et al.* A gene encoding an antigen recognized by cytolytic T lymphocytes on a human melanoma. *Science* 1991; **254**: 1643–7.
- Simpson AJ, Caballero OL, Jungbluth A, Chen YT, Old LJ. Cancer/testis antigens, gametogenesis and cancer. *Nat Rev Cancer* 2005; **5**: 615–25.
- Rosenberg SA, Yang JC, Restifo NP. Cancer immunotherapy: moving beyond current vaccines. *Nat Med* 2004; **10**: 909–15.
- Hattori T, Mine T, Komatsu N *et al.* Immunological evaluation of personalized peptide vaccination in combination with UFT and UZEL for metastatic colorectal carcinoma patients. *Cancer Immunol Immunother* 2009; **58**: 1843–52.
- Noguchi M, Mine T, Komatsu N *et al.* Assessment of immunological biomarkers in patients with advanced cancer treated by personalized peptide vaccination. *Cancer Biol Ther* 2011; **10**: 1266–79.
- Nishikawa H, Kato T, Tawara I *et al.* Accelerated chemically induced tumor development mediated by CD4+CD25+ regulatory T cells in wild-type hosts. *Proc Natl Acad Sci USA* 2005; **102**: 9253–7.
- Nishimura T, Iwakabe K, Sekimoto M *et al.* Distinct role of antigen-specific T helper type 1 (Th1) and Th2 cells in tumor eradication in vivo. *J Exp Med* 1999; **190**: 617–27.
- Takeshima T, Chamoto K, Wakita D *et al.* Local Radiation Therapy Inhibits Tumor Growth through the Generation of Tumor-Specific CTL: its Potentiation by Combination with Th1 Cell Therapy. *Cancer Res* 2010; **70**: 2697–706.
- Hunder NN, Wallen H, Cao J *et al.* Treatment of metastatic melanoma with autologous CD4+ T cells against NY-ESO-1. *N Engl J Med* 2008; **358**: 2698–703.
- Kobayashi H, Celis E. Peptide epitope identification for tumor-reactive CD4 T cells. *Curr Opin Immunol* 2008; **20**: 221–7.
- Kenter GG, Welters MJ, Valentijn AR *et al.* Vaccination against HPV-16 oncoproteins for vulvar intraepithelial neoplasia. *N Engl J Med* 2009; **361**: 1838–47.
- Zwaveling S, Ferreira Mota SC, Nouta J *et al.* Established human papillomavirus type 16-expressing tumors are effectively eradicated following vaccination with long peptides. *J Immunol* 2002; **169**: 350–8.
- Speetjens FM, Kuppen PJ, Welters MJ *et al.* Induction of p53-specific immunity by a p53 synthetic long peptide vaccine in patients treated for metastatic colorectal cancer. *Clin Cancer Res* 2009; **15**: 1086–95.
- Leffers N, Vermeij R, Hoogeboom BN *et al.* Long-term clinical and immunological effects of p53-SLP® vaccine in patients with ovarian cancer. *Int J Cancer* 2011; doi: 10.1002/ijc.25980 [Epub ahead of print].
- Celis E, Center MSGotMCC. Overlapping human leukocyte antigen class I/II binding peptide vaccine for the treatment of patients with stage IV melanoma: evidence of systemic immune dysfunction. *Cancer* 2007; **110**: 203–14.
- Ohkuri T, Wakita D, Chamoto K, Togashi Y, Kitamura H, Nishimura T. Identification of novel helper epitopes of MAGE-A4 tumour antigen: useful tool for the propagation of Th1 cells. *Br J Cancer* 2009; **100**: 1135–43.
- Michaelsen TE, Garred P, Aase A. Human IgG subclass pattern of inducing complement-mediated cytotoxicity depends on antigen concentration and to a lesser extent on epitope patchiness, antibody affinity and complement concentration. *Eur J Immunol* 1991; **21**: 11–6.
- Bijker MS, van den Eeden SJ, Franken KL, Melief CJ, van der Burg SH, Offringa R. Superior induction of anti-tumor CTL immunity by extended peptide vaccines involves prolonged, DC-focused antigen presentation. *Eur J Immunol* 2008; **38**: 1033–42.

## TRIM40 promotes neddylation of IKK $\gamma$ and is downregulated in gastrointestinal cancers

Keita Noguchi<sup>1,2</sup>, Fumihiko Okumura<sup>1</sup>, Norihiko Takahashi<sup>2</sup>, Akhiko Kataoka<sup>2</sup>, Toshiya Kamiyama<sup>2</sup>, Satoru Todo<sup>2</sup> and Shigetsugu Hatakeyama<sup>1,\*</sup>

<sup>1</sup>Department of Biochemistry and <sup>2</sup>Department of General Surgery, Hokkaido University Graduate School of Medicine, N15, W7, Kita-ku, Sapporo, Hokkaido 060-8638, Japan

\*To whom correspondence should be addressed. Tel: +81 11 706 5899; Fax: +81 11 706 5169; Email: hatas@med.hokudai.ac.jp

Gastrointestinal neoplasia seems to be a common consequence of chronic inflammation in the gastrointestinal epithelium. Nuclear factor-kappaB (NF- $\kappa$ B) is an important transcription factor for carcinogenesis in chronic inflammatory diseases and plays a key role in promoting inflammation-associated carcinoma in the gastrointestinal tract. Activation of NF- $\kappa$ B is regulated by several posttranslational modifications including phosphorylation, ubiquitination and neddylation. In this study, we showed that tripartite motif (TRIM) 40 is highly expressed in the gastrointestinal tract and that TRIM40 physically binds to Nedd8, which is conjugated to target proteins by neddylation. We also found that TRIM40 promotes the neddylation of inhibitor of nuclear factor kappaB kinase subunit gamma, which is a crucial regulator for NF- $\kappa$ B activation, and consequently causes inhibition of NF- $\kappa$ B activity, whereas a dominant-negative mutant of TRIM40 lacking the RING domain does not inhibit NF- $\kappa$ B activity. Knockdown of TRIM40 in the small intestinal epithelial cell line IEC-6 caused NF- $\kappa$ B activation followed by increased cell growth. In addition, we found that TRIM40 is highly expressed in normal gastrointestinal epithelia but that TRIM40 is downregulated in gastrointestinal carcinomas and chronic inflammatory lesions of the gastrointestinal tract. These findings suggest that TRIM40 inhibits NF- $\kappa$ B activity via neddylation of inhibitor of nuclear factor kappaB kinase subunit gamma and that TRIM40 prevents inflammation-associated carcinogenesis in the gastrointestinal tract.

### Introduction

Tripartite motif (TRIM) proteins are characterized by the presence of a RING finger, one or two zinc-binding motifs named B-boxes and an associated coiled-coil region (1). Most TRIM proteins have been reported to have a role in the ubiquitination process. TRIM25/estrogen-responsive finger protein ubiquitinates 14-3-3 $\sigma$  (2) and retinoic acid-inducible gene I (3). Furthermore, several TRIM family members are involved in various cellular processes, such as transcriptional regulation, cell growth, apoptosis, development and oncogenesis (4–8).

Neural precursor cell-expressed developmentally downregulated gene 8 (Nedd8) is a small ubiquitin-like protein with 53% identity to ubiquitin that is conserved from yeast to mammals (9–11). Nedd8 is covalently linked to the  $\epsilon$ -amino group of lysine residues on target proteins through its C-terminal group as well as a ubiquitination reaction. Nedd8 is first activated by a heterodimeric E1 enzyme, APPBP1-Uba3 and is then transferred to an E2 enzyme, Ubc12. Members of the cullin family are well-characterized substrates for Nedd8 conjugation (10,12,13). Tumor suppressor protein p53 and its relative p73 are also neddylation via a RING domain containing protein Mdm2 or F-box domain protein FBXO11, and

Abbreviations: cDNA, complementary DNA; IL, interleukin; mRNA, messenger RNA; Nedd8, neural precursor cell-expressed developmentally downregulated gene 8; NF- $\kappa$ B, nuclear factor-kappaB; PBS, phosphate-buffered saline; PCR, polymerase chain reaction; TRIM, tripartite motif.

neddylation of p53 causes inhibition of p53-mediated transcription (14–16). Similarly, c-Cbl mediates epidermal growth factor receptor modification with Nedd8, which enhances subsequent ubiquitination, followed by degradation (17). A well-characterized component of a Cul2-based ubiquitin E3, von Hippel-Lindau protein, is also neddylation, and Nedd8 modification of von Hippel-Lindau protein regulates VHL-associated tumorigenesis (18). Several ribosomal proteins and breast cancer-associated protein3 (BCA3) are modified and regulated by Nedd8 (19,20). Taken together, although neddylation does not directly mediate proteasomal degradation of target proteins like ubiquitination, Nedd8 modification probably regulates several cellular functions including transcription, translation and signal transductions via structural change or stabilization of target proteins.

The nuclear factor-kappaB (NF- $\kappa$ B)-signaling pathway plays a key role in many aspects of cancer initiation and progression through transcriptional control of genes involved in growth, angiogenesis, anti-apoptosis, invasiveness and metastasis (21). Regulation of NF- $\kappa$ B signaling occurs at many levels, one of which is through the regulation of protein turnover by the action of SCF complex ubiquitin ligase. Under a resting condition, NF- $\kappa$ B is maintained in an inactive state by binding to I $\kappa$ B proteins. In canonical NF- $\kappa$ B signaling, I $\kappa$ B $\alpha$  binds to p50-p65 and sequesters transcription factors in the cytoplasm, rendering them inactive. On stimulation of the IKK complex, I $\kappa$ B $\alpha$  is phosphorylated at Serine 32 and Serine 36, resulting in its polyubiquitination by a ubiquitin ligase complex, SCF<sup>Fbw1</sup> (Skp1-Cul1-F-box complex containing Fbw1), and degradation, thus resulting in nuclear accumulation of the complex and transcription of NF- $\kappa$ B target genes (22–25).

Chronic inflammation in the gastrointestinal tract has been closely associated with carcinogenesis (26). The most extensively studied examples are relationships between chronic gastritis resulting from *Helicobacter pylori* infection and gastric cancer, chronic hepatitis and liver cancer and chronic inflammatory bowel disease and colorectal cancer. Emerging evidence in the past decade has suggested that the NF- $\kappa$ B play a critical role in linking inflammation and cancer. NF- $\kappa$ B regulates major inflammatory factors including tumor necrosis factor (TNF)  $\alpha$ , interleukin (IL)-6, IL-1, IL-8, many of which are also potent activators for NF- $\kappa$ B. It is thus probably that NF- $\kappa$ B and inflammation constitute a positive feedback loop in the milieu of inflammatory sites to induce cellular and DNA damage, promote cell proliferation and transformation, and eventually cause initiation, promotion and progression of cancer (27–30).

In this study, we showed that the TRIM family protein TRIM40 is highly expressed in the gastrointestinal tract including the stomach, small intestine and large intestine. With the aim of elucidating the molecular function of TRIM40 in the gastrointestinal tract, we identified Nedd8 as a novel TRIM40-binding protein by using yeast two hybrid screening. TRIM40 enhanced neddylation of IKK $\gamma$  and inhibited the activity of NF- $\kappa$ B-mediated transcription. We also found that knockdown of TRIM40 causes NF- $\kappa$ B activation and increases cell growth. These results provide evidence for a protective role of TRIM40 in inflammation and carcinogenesis in the gastrointestinal tract.

### Materials and methods

#### Cell culture

HEK293T, HeLa and SW480 cell lines were cultured under an atmosphere of 5% CO<sub>2</sub> at 37°C in Dulbecco's modified Eagle's medium (Sigma Chemical Co, St Louis, MO) supplemented with 10% fetal bovine serum (Invitrogen, Carlsbad, CA). IEC-6 cell line was cultured under the same conditions in Dulbecco's modified Eagle's medium supplemented with 10% fetal bovine serum and 0.1 U/ml bovine insulin (Sigma).

### Cloning of complementary DNAs and plasmid construction

Human *TRIM40* complementary DNAs (cDNAs) were amplified from human stomach cDNA by polymerase chain reaction (PCR) with KOD-Plus- (Toyobo, Osaka, Japan) using the following primers: 5'-atgaccccttgcagaaggac-3' (Hs-*TRIM40*-sense) and 5'-tcagagctctgaggggctg-3' (Hs-*TRIM40*-antisense). Mouse *TRIM40* cDNA was amplified from mouse small intestine cDNA by PCR with KOD-Plus- (Toyobo) using the following primers: 5'-accatggctctctgacaaggac-3' (Mm-*TRIM40*-sense) and 5'-agactaactgagcttggaccagc-3' (Mm-*TRIM40*-antisense). The cDNA fragment lacking a sequence corresponding to amino acids 1–54 was utilized as *TRIM40*( $\Delta$ RING). The amplified fragments were subcloned into pBluescript II SK+ (Stratagene, La Jolla, CA). *TRIM40* cDNAs were subcloned into pCR-FLAG, pCGN-HA, pcDNA3-Myc (Invitrogen), pET30a (Merck, Frankfurt, Germany), pGEX-6P1 (GE Healthcare, Piscataway, NJ) and pBTM116 (Clontech, Mountain View, CA). Deletion mutants of mouse *TRIM40* cDNA containing amino acids 55–247 were amplified by PCR and subcloned. Expression vectors encoding IKK $\alpha$ , IKK $\beta$ , IKK $\gamma$  and Nedd8 cDNA were described previously (25).

### Yeast two hybrid screening

cDNA encoding the full length of mouse *TRIM40* was fused in frame to the nucleotide sequence for the LexA domain (Clontech) in the yeast two hybrid vector pBTM116. To screen for proteins that interact with *TRIM40*, we transfected yeast strain L40 (Invitrogen) stably expressing the corresponding pBTM116 vector with a mouse NIH3T3 cDNA library (Clontech).

### Antibodies and reagents

The antibodies used in this study were as follows: mouse monoclonal anti-HA (HA.11/16B12; Covance, Princeton, NJ), rabbit polyclonal anti-HA (Y11; Santa Cruz, Santa Cruz, CA), mouse monoclonal anti-FLAG (M2 or M5; Sigma), mouse monoclonal anti-c-Myc (9E10; Covance), mouse monoclonal anti-human I $\kappa$ B $\alpha$  (610690; BD Pharmingen, San Jose, CA), rabbit polyclonal anti-Nedd8 (PM023; BML, Tokyo, Japan), mouse monoclonal anti-IKK $\gamma$  (K0159-3; BML), mouse monoclonal anti-Hsp70 (610608; BD), mouse monoclonal anti-p65 (610868; BD), mouse monoclonal anti-GAPDH (6C5; Ambion, Austin, TX), mouse monoclonal anti-lamin A/C (612162; BD) and mouse monoclonal anti- $\beta$ -actin (AC15; Sigma). TNF $\alpha$ , IL-1 $\beta$  and cycloheximide were purchased from Sigma.

### Transfection, immunoprecipitation and immunoblot analysis

HEK293T cells were transfected by the calcium phosphate method and lysed in a solution containing 50 mmol/l Tris-HCl (pH 7.4), 150 mmol/l NaCl, 1% Triton X-100, leupeptin (10  $\mu$ g/ml), 1 mmol/l phenylmethylsulfonyl fluoride, 400  $\mu$ mol/l Na<sub>2</sub>VO<sub>4</sub>, 400  $\mu$ mol/l ethylenediaminetetraacetic acid, 10 mmol/l NaF and 10 mmol/l sodium pyrophosphate. The cell lysates were centrifuged at 15 000g for 10 min at 4°C, and the resulting supernatant was incubated with antibodies for 2 h at 4°C. Protein A-sepharose (GE Healthcare) that had equilibrated with the same solution was added to the mixture, which was then rotated for 1 h at 4°C. The resin was separated by centrifugation, washed five times with ice-cold lysis buffer and then boiled in sodium dodecyl sulfate sample buffer. Immunoblot analysis was performed with primary antibodies, horseradish peroxidase-conjugated antibodies to mouse or rabbit IgG (1:10 000 dilution; Promega, Madison, WI) and an enhanced chemiluminescence system (GE Healthcare). Subcellular fractionation was performed as reported previously (31).

### Dual-luciferase assay

HEK293T, HeLa, SW480 and IEC-6 cells were seeded in 24-well plates at 1  $\times$  10<sup>5</sup> cells per well and incubated at 37°C with 5% CO<sub>2</sub> for 24 h. NF- $\kappa$ B luciferase reporter plasmid and pRL-TK Renilla luciferase plasmid (Promega) were transfected into HEK293T, HeLa, SW480 and IEC-6 cells using the Fugene HD reagent (Roche, Basel, Switzerland). Twenty-four hours after transfection, cells were incubated with TNF $\alpha$  (20 ng/ml) for 6 h, harvested and assayed by the Dual-Luciferase Reporter Assay System (Promega). The luminescence was quantified with a luminometer (Tuner Designs, Sunnyvale, CA).

### Immunofluorescence staining

HeLa cells expressing HA-tagged *TRIM40* on a glass cover were fixed by phosphate-buffered saline (PBS) containing 4% formaldehyde and 0.1% Triton X-100 for 10 min at room temperature, followed by incubation with PBS containing anti-HA antibody (Y-11, 1  $\mu$ g/ml), anti-FLAG antibody (M5, 1  $\mu$ g/ml) and anti-p65 antibody (BD, 1  $\mu$ g/ml) with 0.1% bovine serum albumin and 0.1% saponin for 1 h at room temperature. Cells were washed three times with PBS, followed by incubation with PBS containing Alexa546-labeled goat anti-mouse IgG antibody, Alexa488-labeled goat anti-rabbit IgG antibody, Alexa546-labeled goat anti-rabbit IgG antibody or Alexa488-labeled goat anti-mouse IgG antibody (Invitrogen) with 0.1% bovine serum albumin and

0.1% saponin for 1 h at room temperature. The cells were further incubated with Hoechst 33258 (1  $\mu$ g/ml) in PBS for 10 min, followed by extensive washing with PBS and then photographed with a CCD camera (DP71; Olympus, Tokyo, Japan) attached to an Olympus BX51 microscope.

### Recombinant proteins

Glutathione S-transferase-tagged *TRIM40* was expressed in XL-10 cells and then purified by reduced glutathione-sepharose beads (Roche). His<sub>6</sub>/FLAG-tagged *TRIM40* was expressed in *Escherichia coli* strain BL21 (DE3; Invitrogen) and then purified by using ProBond metal affinity beads (Invitrogen).

### Retroviral expression system

Wild-type FLAG-*TRIM40* or FLAG-*TRIM40*( $\Delta$ RING) cDNA was subcloned into pMX-puro. Retroviral expression vectors were kindly provided by Dr Kitamura (University of Tokyo). For retrovirus-mediated gene expression, HeLa cells were infected with retroviruses produced by Plat-A packaging cells. Cells were then cultured in the presence of puromycin (5  $\mu$ g/ml).

### RNA interference

pSUPER-retro-puro containing a non-functional random sequence (5'-cagtcgcgtttgcgactgg-3') or the nucleotides 570–588 of rat *TRIM40* cDNA (5'-cttctctgaggcagtaaca-3') was constructed according to the protocol of the manufacturer (OligoEngine, Seattle, WA). For retrovirus-mediated gene expression, IEC-6 cells were infected with retroviruses produced by Plat-E packaging cells. Cells were then cultured in the presence of puromycin (2  $\mu$ g/ml).

### Quantitative PCR analysis

Total RNA was isolated from human samples with the use of an ISOGEN (Nippon Gene, Tokyo, Japan), followed by reverse transcription by ReverTra Ace (Toyobo). The resulting cDNA was subjected to real-time PCR with a StepOne machine and Power SYBR Green PCR master mix (Applied Biosystems, Foster City, CA). The level of gene expression relative to *GAPDH* was determined. The primer sequences for human *GAPDH* (GenBank accession number NM\_002046.3) and human *TRIM40* (GenBank accession number NM\_138700.3) were as follows: human *GAPDH*, 5'-gcaaatccatggcaccgt-3' and 5'-tcgccccactgattttgg-3' and human *TRIM40*, 5'-caacacactgaagaatgctgg-3' and 5'-cttctgaggggctgaagaag-3'. The primer sequences for rat *GAPDH* (GenBank accession number NM\_017008.3) and rat *TRIM40* (GenBank accession number NM\_001009175.1) were as follows: rat *GAPDH*, 5'-caggcaagtcaacggcaccagta-3' and 5'-gtgaagaccagtagactcaccagc-3' and rat *TRIM40*, 5'-caccggcccactagctc-3' and 5'-ttctgagcctcagccgtg-3'.

### Human tissue samples

Tissues from patients who gave informed consent under the guidelines of the Hokkaido University Hospital Ethics Committee were used for this study. Excised samples from lesions and adjacent normal tissues were obtained within 3 h after the operation. All excised tissues were immediately placed in liquid nitrogen and stored at –80°C until further analysis.

### Statistical analysis

The unpaired Student's *t*-test and Wilcoxon matched pairs test were used to determine the statistical significance of experimental data.

## Results

### *TRIM40* expression in normal mouse tissues and mammalian cell lines

We and others have shown that some of the TRIM family members are selectively expressed in specific tissues and cell lines (1,6,7). Although several TRIM family members are known to be involved in various cellular processes, the functions of almost all TRIM family proteins have not been elucidated. In this study, we found human and mouse *TRIM40* as a new member of the TRIM family and we analyzed the biological function of *TRIM40*. To examine the expression levels of *TRIM40* in several normal tissues at the protein level, we generated a rabbit polyclonal anti-*TRIM40* antibody using recombinant mouse *TRIM40* protein and performed immunoblot analysis using several mouse normal tissues. Immunoblot analysis showed that *TRIM40* is highly expressed in the gastrointestinal tract, heart and cerebellum and faintly in the testis (Figure 1A). To further analyze the expression of *TRIM40* in detail, we prepared several gastrointestinal tissues including the esophagus, stomach, small intestine and large intestine. Immunoblot analysis using cell extracts from these tissues showed that *TRIM40* is expressed highly in the small intestine, moderately in the stomach and faintly in the esophagus and large intestine

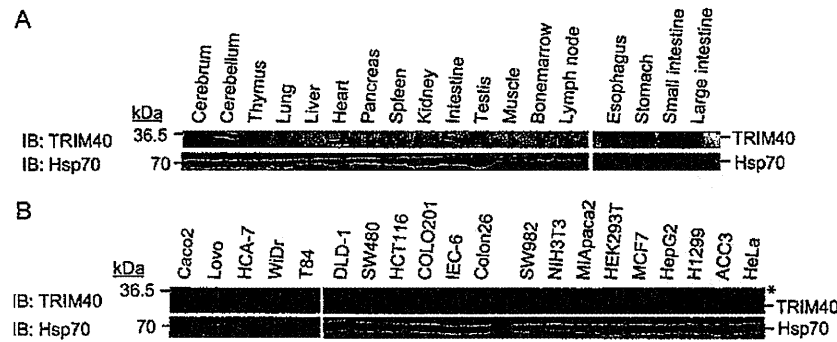


**Fig. 1.** Expression levels of TRIM40 in several mouse tissues and cell lines. (A) TRIM40 expression in several mouse tissues. The lysates from indicated mouse tissues were subjected to immunoblot (IB) analysis with anti-TRIM40 antibody and anti-Hsp70 antibody as a loading control. (B) TRIM40 expression in several cell lines. IB analysis with anti-TRIM40 or anti-Hsp70 antibody was performed using cell lysates from human intestine epithelial carcinoma cell lines Caco2, Lovo, HCA-7, WiDr, T84, DLD-1, SW480, HCT116 and COLO201, rat intestine epithelial cell line IEC-6, mouse colon epithelial carcinoma cell line Colon26, human synovial sarcoma cell line SW982, mouse embryonic fibroblast cell line NIH3T3, human pancreatic adenocarcinoma cell line MIApaca 2, human embryonic kidney cell line HEK293T, human breast carcinoma cell line MCF7, human hepatocellular carcinoma cell line HepG2, human lung carcinoma cell line H1299, human adenoid cystic carcinoma cell line ACC3 and human cervical carcinoma cell line HeLa. Asterisk represents non-specific band.

(Figure 1A). Furthermore, immunoblot analysis using several cell lines showed that TRIM40 is highly expressed in the rat small intestinal epithelial cell line IEC-6, the mouse colon adenocarcinoma cell line Colon26 and the human adenoid cystic carcinoma cell line ACC3, which are developmentally derived from parotid glands or gastrointestinal tissues (Figure 1B). These findings suggest that TRIM40 is more highly expressed in normal intestinal cells than in intestinal carcinoma cells.

#### TRIM40 interacts with Nedd8

To examine the molecular function of TRIM40, we isolated TRIM40-interacting proteins from an NIH 3T3 cDNA library by using a yeast two hybrid system. We obtained 16 positive clones from  $1.2 \times 10^6$  transformants. Eight of the positive clones had sequence identities with cDNA encoding mouse Nedd8 (NCBI Reference Sequence: NM\_008683.3). To examine whether TRIM40 physically interacts with Nedd8 in mammalian cells, we performed an *in vivo*-binding assay using cells transfected with expression vectors. We expressed FLAG-tagged TRIM40 together with Myc-tagged Nedd8 in HEK293T cells. Cell lysates were subjected to immunoprecipitation with an antibody to FLAG, and the resulting precipitates were subjected to immunoblot analysis with an antibody to Myc. Myc-tagged Nedd8 was coprecipitated by the antibody to FLAG, indicating that TRIM40 non-covalently interacts specifically with Nedd8 and also is covalently conjugated with Nedd8 (neddylation) (Figure 2A). We also confirmed interaction between FLAG-tagged TRIM40 lacking a RING domain [TRIM40( $\Delta$ RING)] and Myc-tagged Nedd8 by immunoprecipitation, suggesting that TRIM40( $\Delta$ RING) can be used as a null-functional mutant or a dominant-negative mutant (Figure 2A). Furthermore, immunoblot analysis using anti-Nedd8 antibody showed that overexpressed FLAG-tagged TRIM40 is covalently conjugated with Nedd8, but we could not show that overexpressed FLAG-tagged TRIM40 non-covalently interacts with Nedd8 (Figure 2A and B). These findings suggest that TRIM40 is covalently conjugated with Nedd8 and that TRIM40 weakly interacts with monomeric Nedd8.

#### TRIM40 inhibits NF- $\kappa$ B activity

It has been reported that Nedd8 covalently binds to and activates Cull1, which is a component of an SCF complex and that the SCF complex degrades I $\kappa$ B $\alpha$  phosphorylated by stimulation of TNF $\alpha$ , followed the activation of NF- $\kappa$ B-mediated transcription (12,13). To examine whether TRIM40 affects NF- $\kappa$ B activity, we performed an NF- $\kappa$ B response element luciferase reporter assay. We transfected expression vectors encoding TRIM40 with reporter plasmids into HEK293T cells. Six hours after stimulation with TNF $\alpha$ , luciferase activity was measured. The luciferase assays showed that TRIM40 suppressed

NF- $\kappa$ B-mediated transcriptional activity in a dose-dependent fashion (Figure 2C). Furthermore, stable HeLa cell lines expressing FLAG-tagged TRIM40(WT) and FLAG-TRIM40( $\Delta$ RING) were generated by a retroviral expression system and luciferase assays were performed using these cell lines. Luciferase assays showed that overexpression of TRIM40 inhibits NF- $\kappa$ B activity compared with that of Mock, whereas overexpression of TRIM40( $\Delta$ RING) does not affect NF- $\kappa$ B activity, suggesting that a RING domain of TRIM40 is indispensable for inhibition of NF- $\kappa$ B activity (Figure 2D and E). In addition, we showed that TRIM40 also suppressed TNF $\alpha$ -induced NF- $\kappa$ B activity using the human colorectal adenocarcinoma cell line SW480 (Figure 2F). Since a canonical NF- $\kappa$ B pathway can be activated by many stimulations including stimulations with TNF $\alpha$ , IL-1 $\beta$  and lipopolysaccharide, a luciferase reporter assay using IL-1 $\beta$  was performed. The luciferase reporter assay showed that TRIM40 suppressed IL-1 $\beta$ -induced NF- $\kappa$ B activity (Figure 2G). These findings suggest that TRIM40 downregulates NF- $\kappa$ B-mediated transcriptional activity.

#### TRIM40 inhibits nuclear translocation of NF- $\kappa$ B

It has been reported that the p65 subunit of NF- $\kappa$ B is translocated from the cytoplasm to the nucleus upon stimulation with TNF $\alpha$  (32). To examine whether TRIM40 affects nuclear translocation of p65, immunofluorescent analysis was performed using an anti-p65 antibody. An expression vector encoding HA-tagged TRIM40 was transfected into HeLa cells, and the cells were stimulated with TNF $\alpha$  for 20 or 30 min and then stained with anti-p65 antibody. It was found that p65 was concentrated in the nucleus of mock cells by treatment with TNF $\alpha$ , whereas p65 was weakly concentrated in the nucleus of cells in which TRIM40 was highly expressed (Figure 3A and B). Immunofluorescent staining showed that overexpression of TRIM40 inhibits nuclear localization of endogenous p65 in HeLa cells by stimulation with TNF $\alpha$ , suggesting that TRIM40 inhibits a canonical NF- $\kappa$ B pathway (Figure 3A and B). The effect of TRIM40 on nuclear localization of endogenous p65 by TNF $\alpha$  was further confirmed by biochemical subcellular fractionation of HeLa cells. Immunoblotting with anti-p65 antibody was performed using each subcellular fraction from cells stimulated with TNF $\alpha$ . Endogenous p65 was mainly localized in the nucleus in mock cells by stimulation with TNF $\alpha$ , whereas half of the endogenous p65 remained in the cytosol in TRIM40-expressing cells, suggesting that TRIM40 inhibits nuclear translocation of p65 induced by stimulation with TNF $\alpha$  (Figure 3C and D).

#### TRIM40 stabilizes I $\kappa$ B $\alpha$ and interacts with IKK complex

Since we found that TRIM40 inhibits nuclear translocation of NF- $\kappa$ B and NF- $\kappa$ B-mediated transcriptional activity, we hypothesized that overexpression of TRIM40 would inhibit degradation of I $\kappa$ B $\alpha$ . To

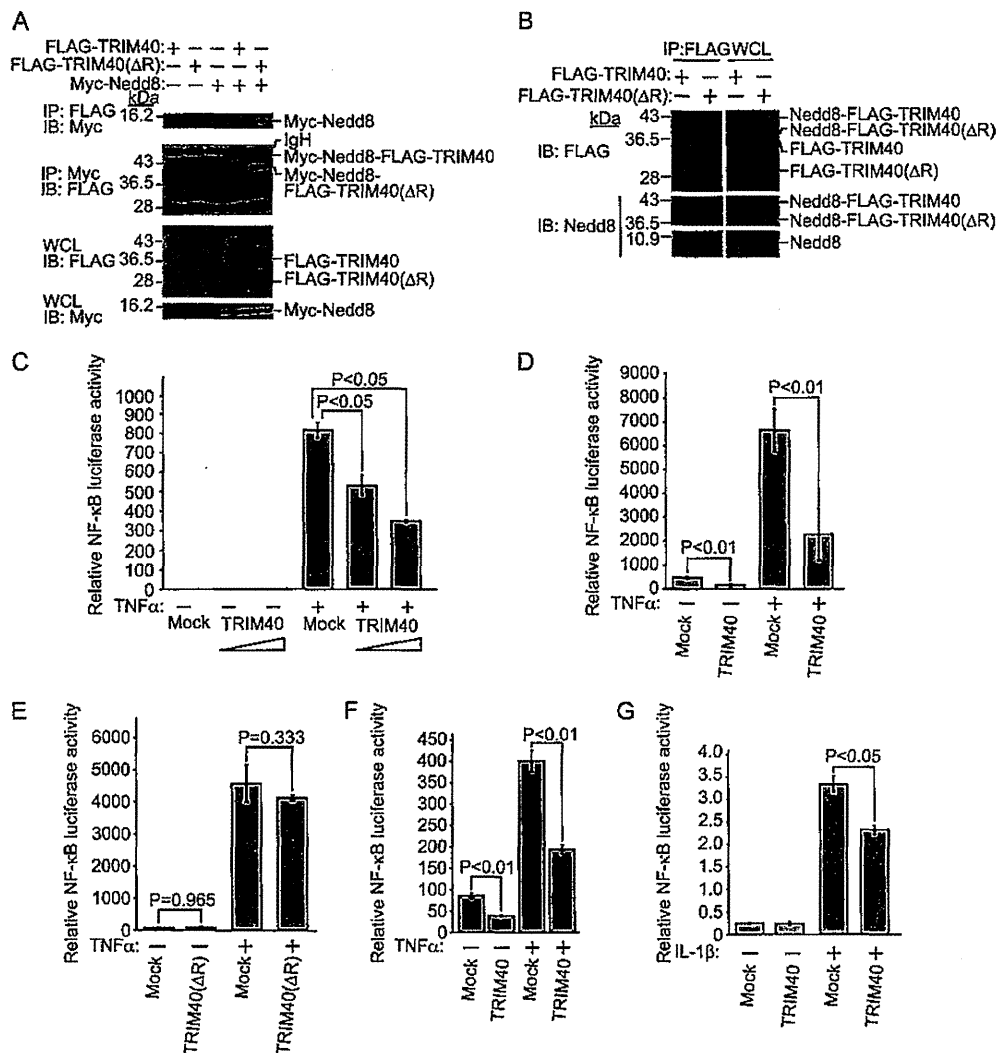


**Fig. 2.** TRIM40 interacts with Nedd8 and downregulates NF-κB activity. (A) *In vivo*-binding assay between TRIM40 and Nedd8. Expression vectors encoding FLAG-tagged TRIM40, FLAG-tagged TRIM40(ΔR) and Myc-tagged Nedd8 were transfected into HEK293T cells. Cell lysates (WCL) were immunoprecipitated with anti-FLAG or anti-Myc antibody and immunoblotted with anti-Myc and anti-FLAG antibodies. (B) *In vivo*-binding assay between TRIM40 and Nedd8. Expression vectors encoding FLAG-tagged TRIM40 and FLAG-tagged TRIM40(ΔR) were transfected into HEK293T cells. Cell lysates (WCL) were immunoprecipitated with anti-FLAG antibody and immunoblotted with anti-FLAG and anti-Nedd8 antibodies. (C) TRIM40 reduces TNFα-induced NF-κB activity in a dose-dependent manner. HEK293T cells were transfected with the NF-κB luciferase reporter plasmid and an expression plasmid encoding TRIM40 (100 or 300 ng). Twenty-four hours after transfection, cells were treated with TNFα (20 ng/μl) and cultured for an additional 6 h. Data are means ± standard deviation of values from three independent experiments. The *P* values for the indicated comparisons were determined by Student's *t*-test. (D) Luciferase assay for NF-κB activity using HeLa cell lines stably expressing FLAG-tagged TRIM40. Stable cell lines were transfected with the NF-κB luciferase reporter plasmid. Twenty-four hours after transfection, cells were treated with TNFα (20 ng/μl) and cultured for an additional 6 h. (E) Luciferase assay for NF-κB activity using HeLa cell lines stably expressing FLAG-tagged TRIM40(ΔRING). Stable cell lines were transfected with the NF-κB luciferase reporter plasmid. Twenty-four hours after transfection, cells were treated with TNFα (20 ng/μl) and cultured for an additional 6 h and then luciferase activity was measured. R, RING domain. (F) TRIM40 reduces TNFα-induced NF-κB activity in the human colorectal adenocarcinoma cell line SW480. SW480 cells were transfected with the NF-κB luciferase reporter plasmid and an expression plasmid encoding TRIM40 (300 ng). Twenty-four hours after transfection, cells were treated with TNFα (20 ng/μl) and cultured for an additional 6 h and then luciferase activity was measured. (G) TRIM40 reduces IL-1β-induced NF-κB activity. HEK293T cells were transfected with the NF-κB luciferase reporter plasmid and an expression plasmid encoding TRIM40 (300 ng). Twenty-four hours after transfection, cells were treated with IL-1β (10 ng/μl) and cultured for an additional 6 h and then luciferase activity was measured.

examine whether overexpression of TRIM40 affects the stability of IκBα, an expression vector encoding TRIM40 was transfected. Immunoblot analysis clarified that overexpression of TRIM40 increases the stability of IκBα (Figure 4A). To further confirm that TRIM40 affects the stability of IκBα, a protein stability assay using cycloheximide was performed. HeLa cell lines stably expressing FLAG-tagged TRIM40 were stimulated with TNFα and incubated with cycloheximide for 0–60 min. The protein stability assay showed that stimula-

tion with TNFα did not completely degrade IκBα even after 20 min of stimulation, suggesting that TRIM40 suppressed TNF-induced IκBα degradation (Figure 4B and C).

Next, we tested whether TRIM40 interacts with IKKα, IKKβ and IKKγ as upstream regulators for IκBα. We transfected expression vectors encoding HA-tagged TRIM40 or HA-tagged TRIM40(ΔRING) and FLAG-tagged IKKα, FLAG-tagged IKKβ or FLAG-tagged IKKγ into HEK293T cells. Cell lysates were

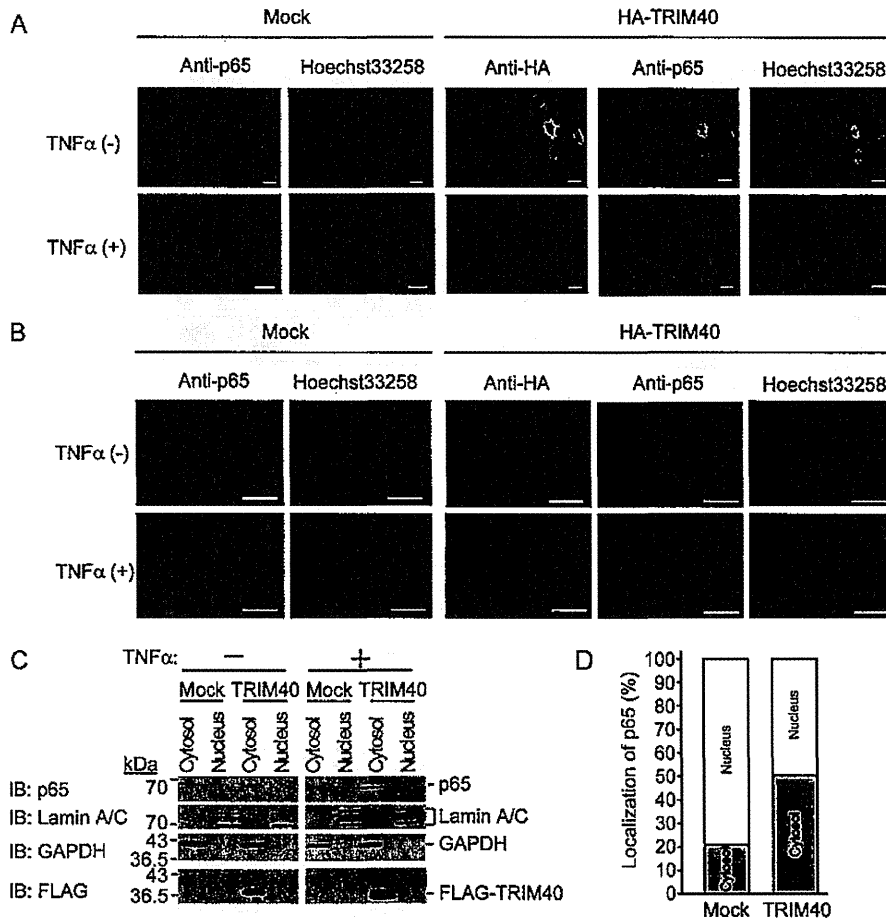


**Fig. 3.** TRIM40 inhibits translocation of p65 from the cytosol to the nucleus. (A) Immunofluorescent staining of p65 in TRIM40-overexpressing cells at low magnification. HeLa cells were transfected with an expression plasmid encoding HA-tagged TRIM40. Forty-eight hours after transfection, the cells were stimulated with TNF $\alpha$  (20 ng/ml) for 20 min and were stained with anti-HA and anti-p65 antibodies, followed by incubation with Alexa488-labeled anti-rabbit IgG antibody and Alexa546-labeled anti-mouse IgG antibody, respectively. Nuclei were visualized using Hoechst 33258. Scale bars, 10  $\mu$ m. (B) Immunofluorescent staining of p65 in TRIM40-overexpressing cells at high magnification. HeLa cells were transfected with an expression plasmid encoding HA-tagged TRIM40. Forty-eight hours after transfection, the cells were stimulated with TNF $\alpha$  (20 ng/ml) for 30 min and were stained with anti-HA and anti-p65 antibodies, followed by incubation with Alexa546-labeled anti-rabbit IgG antibody and Alexa488-labeled anti-mouse IgG antibody, respectively. Nuclei were visualized using Hoechst 33258. Scale bars, 10  $\mu$ m. (C) Subcellular fractionation of p65 from TRIM40-overexpressing cells. HeLa cell lines stably expressing FLAG-tagged TRIM40 were stimulated with TNF $\alpha$  (20 ng/ml). Thirty minutes after stimulation, biochemically fractionated cytosolic and nuclear extracts were subjected to immunoblot analysis with anti-p65, anti-GAPDH and anti-Lamin A/C antibodies. GAPDH and lamin A/C are used as cytosolic and nuclear markers, respectively. (D) Quantification of p65 in cytosol or nuclear fractions. The intensities of p65 bands in (C) were quantified using a densitometer.

subjected to immunoprecipitation with an antibody to HA or FLAG, and the resulting precipitates were subjected to immunoblot analysis with an antibody to FLAG or HA, respectively. Immunoblot analysis showed that HA-tagged TRIM40 was selectively coprecipitated by anti-FLAG antibody and that FLAG-tagged IKK $\alpha$ , FLAG-tagged IKK $\beta$  and FLAG-tagged IKK $\gamma$  were also coprecipitated by anti-HA antibody (Figure 4D, E and F). We also verified interaction between HA-tagged TRIM40( $\Delta$ RING) and FLAG-tagged IKK $\alpha$ , FLAG-tagged IKK $\beta$  or FLAG-tagged IKK $\gamma$  by immunoprecipitation (Figure 4D, E and F). TRIM40( $\Delta$ R) interacts with IKK subunits much more strongly than TRIM40(WT) does (Figure 4D, E and F), suggesting that the RING domain may inhibit the interaction between TRIM40 and IKK subunits. These findings suggest that TRIM40 is contained in the IKK complex and inhibits the degradation of I $\kappa$ B $\alpha$  in a resting state.

#### TRIM40 is modified by Nedd8 and promotes neddylation of IKK $\gamma$

It has been reported that IKK $\gamma$  is regulated by several posttranslational modifications including K63-linked or linear polyubiquitination

(33,34). Since TRIM40 interacts with Nedd8 and IKK $\gamma$ , we examined whether Nedd8 affects IKK $\gamma$  by TRIM40. To examine whether TRIM40 exhibits Nedd8 conjugation on IKK $\gamma$ , we performed an *in vivo* neddylation assay. Expression vectors encoding FLAG-tagged IKK $\gamma$ , HA-tagged TRIM40, HA-tagged TRIM40( $\Delta$ RING) and Myc-tagged Nedd8 were transfected into HEK293T cells, and cell lysates were subjected to immunoprecipitation with an antibody to Myc and immunoblotted with an antibody to FLAG. Although FLAG-IKK $\gamma$  was slightly neddylated even without overexpression of TRIM40, overexpression of TRIM40 considerably enhanced neddylation of FLAG-IKK $\gamma$  (Figure 5A). Next, to elucidate in detail whether TRIM40 neddylates IKK $\gamma$ , we performed an *in vivo* neddylation assay using several amounts of an expression vector HA-tagged TRIM40. Immunoblot analysis showed that TRIM40 enhances neddylation on IKK $\gamma$  in a dose-dependent fashion (Figure 5B), suggesting that TRIM40 mediates neddylation on IKK $\gamma$  and then possibly modulates kinase activity of the IKK complex, followed by stabilization of I $\kappa$ B $\alpha$ . Although immunoblot analysis of IKK $\alpha$  and IKK $\beta$  was



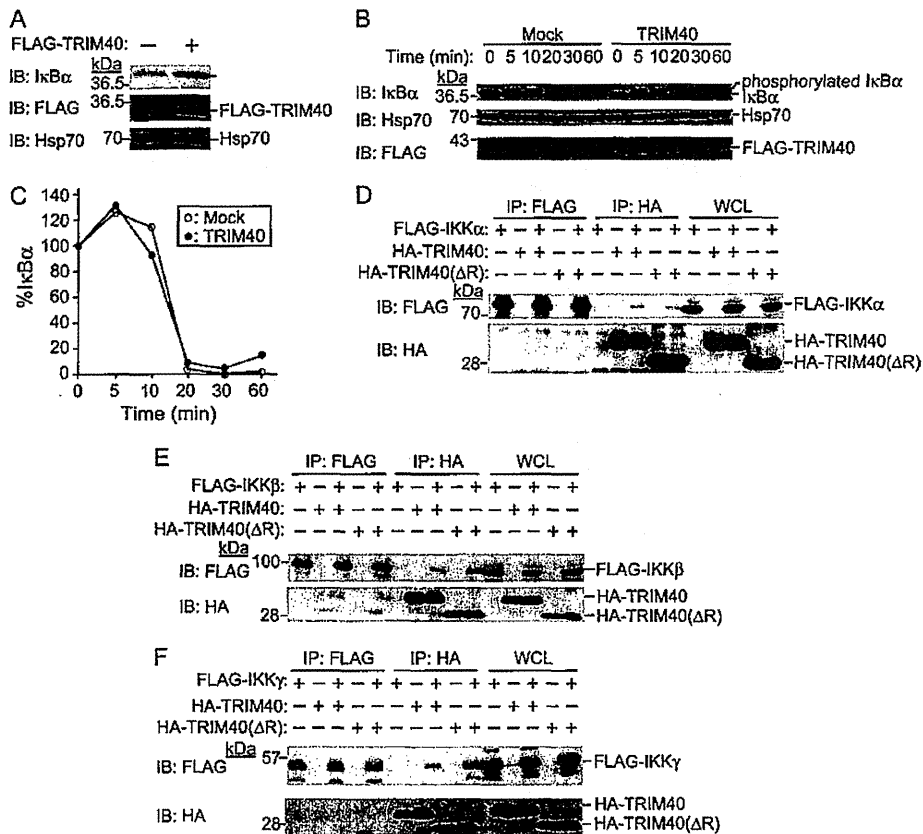


**Fig. 4.** TRIM40 interacts with IKK complex. (A) Upregulation of endogenous IκBα by TRIM40. Immunoblot analysis was performed using HeLa cells stably expressing FLAG-tagged TRIM40. Cell lysates were subjected to immunoblot (IB) analysis with anti-FLAG, anti-IκBα or anti-Hsp70 antibody. Anti-Hsp70 antibody was used as a loading control. (B) TRIM40 affects the stability of IκBα. HeLa cell lines stably expressing FLAG-tagged TRIM40 were stimulated with TNFα (20 ng/ml) and cycloheximide (25 μg/ml) for 0–60 min. Cell extracts were analyzed by immunoblotting with anti-IκBα antibody, anti-Hsp70 antibody and anti-FLAG antibody. Anti-Hsp70 antibody was used as a loading control. (C) Intensity of the IκBα bands in protein stability analysis in (B) was normalized by that of the corresponding Hsp70 bands and was then expressed as a percentage of the normalized value for time zero. (D) Interaction between IKKα and TRIM40. HEK293T cells were transfected with plasmids encoding FLAG-tagged IKKα, HA-tagged TRIM40 and HA-tagged TRIM40(ΔRING), followed by immunoprecipitation (IP) with anti-FLAG antibody or anti-HA antibody. Immunoprecipitates were subjected to IB analysis with anti-FLAG or anti-HA antibody. (E) Interaction between IKKβ and TRIM40. HEK293T cells were transfected with plasmids encoding FLAG-tagged IKKβ, HA-tagged TRIM40 and HA-tagged TRIM40(ΔRING), followed by IP with anti-FLAG antibody or anti-HA antibody. Immunoprecipitates were subjected to IB analysis with anti-FLAG or anti-HA antibody. (F) Interaction between IKKγ and TRIM40. HEK293T cells were transfected with plasmids encoding FLAG-tagged IKKγ, HA-tagged TRIM40 and HA-tagged TRIM40(ΔRING), followed by IP with anti-FLAG antibody or anti-HA antibody. Immunoprecipitates were subjected to IB analysis with anti-FLAG or anti-HA antibody.

performed, neddylation of IKKα and IKKβ was not observed (Figure 5C and D).

**Knockdown of TRIM40 promotes activity of NF-κB and increases cell growth**

To evaluate the physiological function of TRIM40, retroviral vectors encoding shRNA specific for rat TRIM40 (shTRIM40) or non-targeting shRNA as a control (Mock) were infected into IEC-6 cells in which TRIM40 is highly expressed. After puromycin selection, a stable IEC-6 cell line in which TRIM40 is knocked down was established, and TRIM40 expression at protein and messenger RNA (mRNA) levels was confirmed by immunoblot analysis and quantitative real-time PCR, respectively (Figure 6A and B). Using these cell lines, we performed an NF-κB response element luciferase reporter assay. Six hours after stimulation with TNFα, luciferase activity was measured. The luciferase assays showed that knockdown of TRIM40 enhances NF-κB-mediated transcriptional activity (Figure 6C). Interestingly, knockdown of TRIM40 caused activation of NF-κB-mediated transcription even without TNFα stimulation. In addition, knockdown of TRIM40 increased cell growth (Figure 6D). These findings suggest that TRIM40 downregulates NF-κB-mediated tran-

scriptional activity and that TRIM40 is an important regulator to prevent NF-κB activation in a resting state.

Since it has been reported that NF-κB activity is upregulated in gastrointestinal carcinomas, we investigated the expression of TRIM40 mRNA in human cancers and inflammation (29,30). Quantitative real-time PCR was performed and mRNA expression levels of TRIM40 were compared in gastrointestinal cancers (including Crohn's disease) and normal tissues. Expression levels of TRIM40 mRNA were lower in samples of gastric cancer (13/13), colon cancer (3/3), rectal cancer (3/4), benign colon tumor (0/1) and Crohn's disease (1/1) than in normal epithelia. Quantitative real-time PCR showed that TRIM40 mRNA is highly expressed in human normal gastrointestinal tissues and significantly downregulated in gastrointestinal carcinomas and inflammation (Figure 6E and F).

To verify Nedd8 conjugation of IKKγ in human gastrointestinal tissues, immunoprecipitation and immunoblot analysis were performed using normal gastric epithelium and gastric cancer tissue from the same patient. Cell lysates were subjected to immunoprecipitation with an antibody to anti-IKKγ or anti-Nedd8, and the resulting precipitates were subjected to immunoblot analysis with an antibody to anti-Nedd8 or anti-IKKγ, respectively. Neddylation of IKKγ was selectively detected in normal gastric epithelium (Figure 6F). These

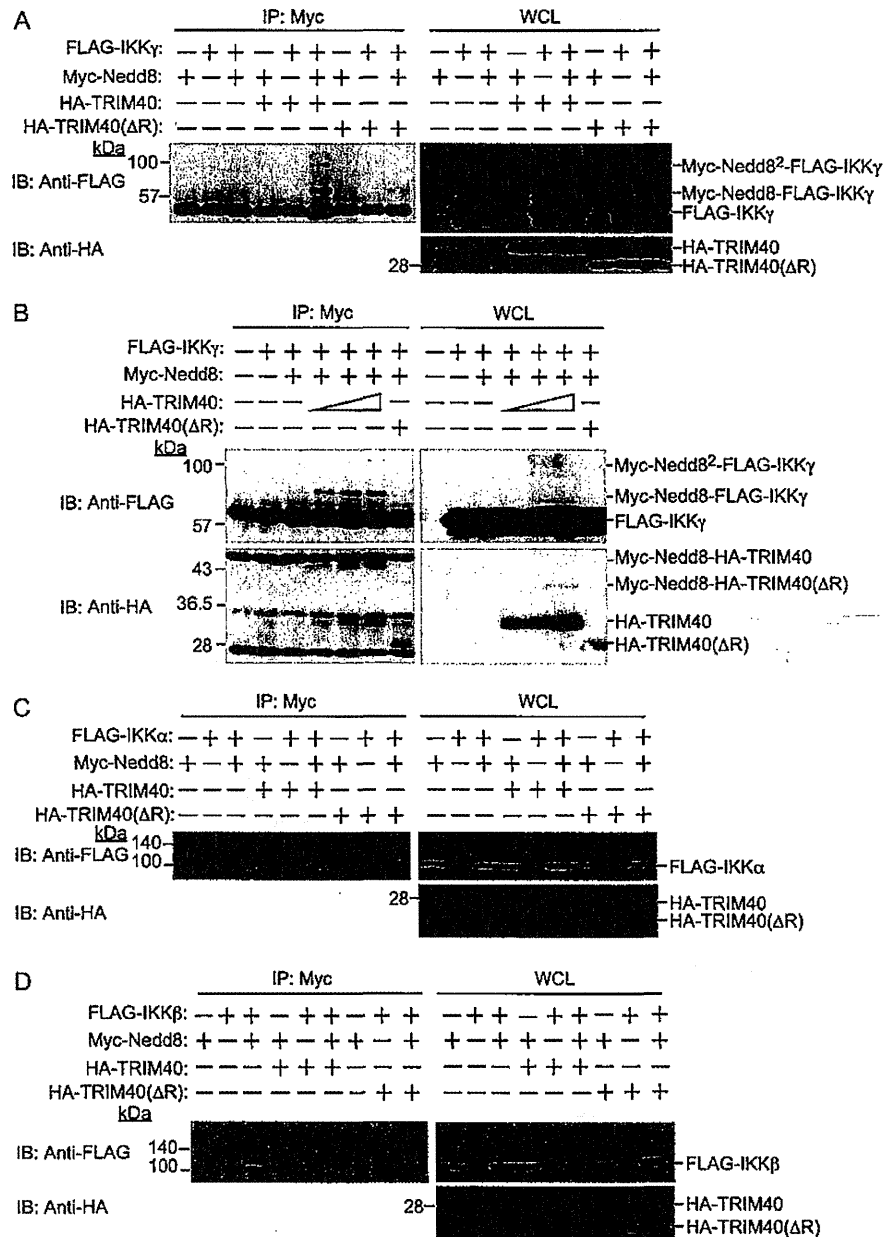


**Fig. 5.** TRIM40 promotes neddylation of IKK $\gamma$ . (A) *In vivo* neddylation assay of IKK $\gamma$  by TRIM40. HEK293T cells were transfected with plasmids encoding FLAG-tagged IKK $\gamma$ , HA-tagged TRIM40, HA-tagged TRIM40 ( $\Delta$ RING) and Myc-tagged Nedd8, followed by immunoprecipitation (IP) with anti-Myc antibody. Immunoprecipitates were subjected to immunoblot (IB) analysis with anti-FLAG or anti-HA antibody. (B) TRIM40 promotes neddylation of IKK $\gamma$  in a dose-dependent fashion. HEK293T cells were transfected with plasmids encoding FLAG-IKK $\gamma$ , HA-TRIM40 (1, 3 or 6  $\mu$ g), HA-tagged TRIM40( $\Delta$ RING) (3  $\mu$ g) and Myc-tagged Nedd8, followed by IP with anti-Myc antibody. Immunoprecipitates were subjected to IB analysis with anti-FLAG or anti-HA antibody. (C and D) *In vivo* neddylation assay of IKK $\alpha$  or IKK $\beta$  by TRIM40. HEK293T cells were transfected with plasmids encoding FLAG-tagged IKK $\alpha$  or IKK $\beta$ , HA-tagged TRIM40, HA-tagged TRIM40 ( $\Delta$ RING) and Myc-tagged Nedd8, followed by IP with anti-Myc antibody. Immunoprecipitates were subjected to IB analysis with anti-FLAG or anti-HA antibody.

findings suggest that endogenous TRIM40 is highly expressed and promotes neddylation of IKK $\gamma$ , resulting in stabilization of I $\kappa$ B $\alpha$ .

## Discussion

In this study, we found that TRIM40 is highly expressed in gastrointestinal tissues and that TRIM40 interacts with the ubiquitin-like protein Nedd8. We focused on the relationship between TRIM40 and Nedd8 because Nedd8 conjugation regulates activity of NF- $\kappa$ B

through the SCF complex (12). Although it has been reported that a subunit of SCF complex, Cul1, is positively regulated via Nedd8 conjugation, we did not find interaction of TRIM40 with the SCF complex (data not shown). We further investigated other steps for NF- $\kappa$ B activation and found that TRIM40 interacts with the IKK complex. We showed that overexpression of TRIM40 promotes neddylation of IKK $\gamma$  and that TRIM40 causes stabilization of I $\kappa$ B $\alpha$  and attenuates NF- $\kappa$ B activity, whereas a mutant of TRIM40 lacking the RING-finger domain does not affect NF- $\kappa$ B activity. Furthermore,

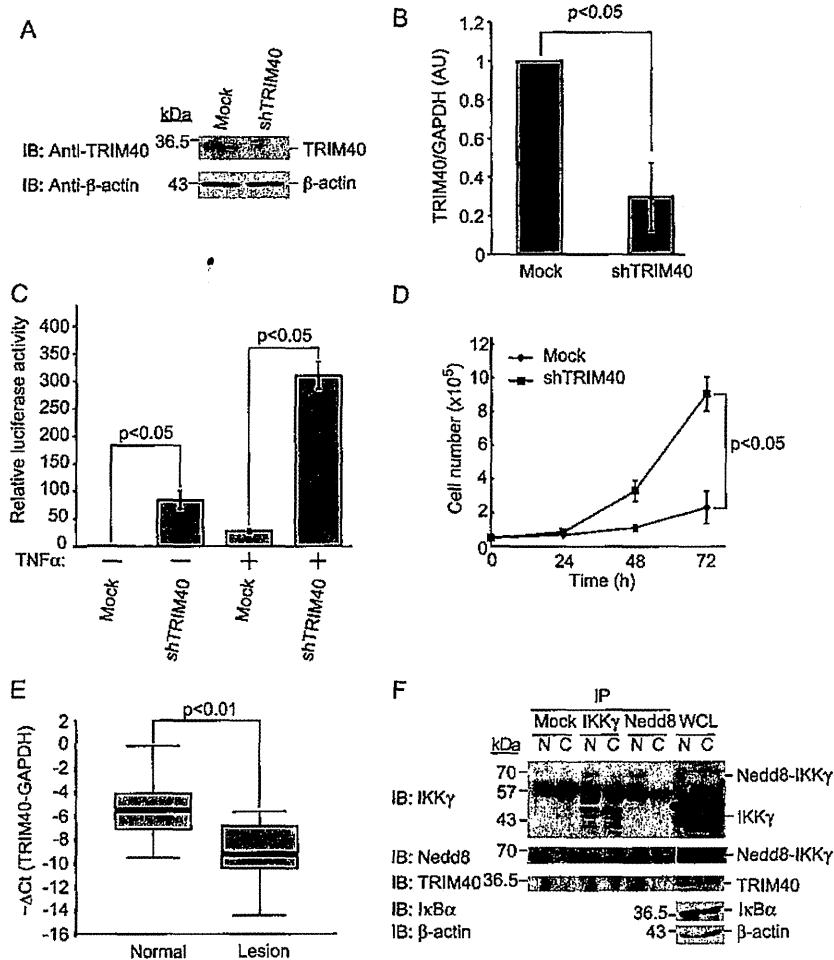


**Fig. 6.** Knockdown of TRIM40 promotes NF-κB-mediated transcription and accelerates cell growth. (A) Establishment of stably knocked-down IEC-6 cell lines with shRNA specific for rat *TRIM40* (shTRIM40) or with non-targeting shRNA as a control (Mock). Immunoblot analysis was performed with anti-TRIM40 or anti-β-actin antibody. (B) *TRIM40* mRNA expression in stably knocked-down IEC-6 cell lines with shRNA specific for rat *TRIM40* (shTRIM40) or with non-targeting shRNA as a control (Mock). *TRIM40* mRNA levels in these cell lines were measured by quantitative real-time PCR. (C) Knockdown of TRIM40 enhances NF-κB-mediated transcription. Stably knocked-down cells were transfected with the NF-κB luciferase reporter plasmid. Twenty-four hours after transfection, cells were treated with TNFα (20 ng/μl) and cultured for an additional 6 h and then luciferase activity was measured. Data are means ± standard deviation of values from three independent experiments. (D) Knockdown of TRIM40 causes growth delay of IEC-6 cells. Cell lines were seeded at 5 × 10<sup>4</sup> cells in six-well plates and harvested for determination of cell number at indicated times. Data are means ± standard deviation of values from three independent experiments. (E) TRIM40 is downregulated in human gastrointestinal carcinomas. *TRIM40* mRNA levels in human gastrointestinal diseases and adjacent normal tissues from 22 cases were compared by quantitative real-time PCR. The expression level of *TRIM40* mRNA was normalized to that of *GAPDH* mRNA and shown as relative expression level. The boxes within the plots represent the 25–75th percentiles. The horizontal line in the boxes indicates median value. The *P* values for the indicated comparisons were determined by Wilcoxon matched pairs test. Samples used in this assay were as follows: gastric cancers, 13; colon cancer, 3; rectal cancer, 4; benign colon tumor, 1; Crohn’s disease, 1. (F) Nedd8ylation of IKKγ in gastric cancer sample. Cell lysates were subjected to immunoprecipitation with an antibody to IKKγ or anti-Nedd8, and the resulting precipitates were subjected to immunoblot analysis with an antibody to anti-IKKγ, anti-TRIM40 or anti-Nedd8. N, normal tissues; C, cancer tissues.

knockdown of TRIM40 promoted NF-κB activity and cell growth. Taken together, these results suggest that TRIM40 is a novel-negative regulator against inflammation and carcinogenesis in the gastrointestinal tract.

It has been reported that the E3 ubiquitin ligase MDM2 promotes neddylation of p53 and negatively regulates its transcriptional activity (14) and that an F-box protein, FBXO11, which is a component of the SCF type E3 ligase, promotes neddylation of p53 and inhibits its transcriptional activity (16). Therefore, we hypothesized that TRIM40 promotes neddylation of IKKγ via a RING domain and regulates the activity of IKK complex, in which IKKγ is an essential component for activation of the canonical NF-κB pathway. Non-proteolytic lysine 63 (K63)-linked polyubiquitination has as an important role in IKK activation in the canonical NF-κB pathway (35). IKKγ specifically rec-

ognizes K63-linked polyubiquitin chains and is conjugated by K63-linked polyubiquitin chains, which induces activation of the IKK complex and promotes the NF-κB cascade (33,36,37). In addition, IKKγ is conjugated by N-terminal-linked linear polyubiquitin chains and linear polyubiquitin of IKKγ is necessary for an NF-κB pathway (34). In this study, we showed that overexpression of TRIM40 results in neddylation of IKKγ and inhibition of NF-κB activity and that knockdown of TRIM40 accelerates NF-κB activity and cell growth. Taken together, these findings indicate that non-proteolytic polyubiquitin chains by K63-linked and linear types on IKKγ positively regulate the IKK complex, whereas Nedd8 conjugation of IKKγ probably functions as a negative regulator for NF-κB activity.

Intestinal epithelial cells provide a primary physical barrier against commensal and pathogenic microorganisms in the gastrointestinal

tract, but the influence of intestinal epithelial cells on the development and regulation of immunity to infection is unknown (38). Many kinds of enterobacteria exist in the gastrointestinal tract. Despite the fact that enterobacteria are non-self antigens, the intestinal tract has no immune response for enterobacteria. The normal intestinal tract seems to have an immune suppression system for enterobacteria. In particular, chronic inflammation by pathogenic bacteria such as *H.pylori* or inflammatory bowel diseases including Crohn's disease and ulcerative colitis are closely associated with cancer (26). Evidence that has accumulated in the past decade has suggested that NF- $\kappa$ B plays a critical role in linking inflammation and cancer (27–30). Tissue reconstruction by chronic inflammation may induce malignant transformation of the gastrointestinal epithelium. Therefore, appropriate regulation of immune responses in the gastrointestinal tract, in which various bacteria cause inflammation, may be required for preventing carcinogenesis. We showed that TRIM40 is highly expressed in normal gastrointestinal epithelia compared with the expression level in inflammatory gastrointestinal tracts and cancer lesions. TRIM40 may downregulate production of inflammatory cytokines including TNF $\alpha$ , IL-6, IL-1, IL-8 via inhibition of NF- $\kappa$ B and prevent carcinogenesis through inflammation by enteric bacteria. Hence, TRIM40 may function as an important regulator for maintaining homeostasis of the gastrointestinal tract.

Dysregulation of NF- $\kappa$ B is involved in the etiology of cancer and leukemia. Recently, NF- $\kappa$ B has attracted attention as a target of drugs for cancer and immune regulation. The proteasome inhibitor Bortezomib, one function of which is NF- $\kappa$ B inhibition through reduced I $\kappa$ B degradation, leading to reduced NF- $\kappa$ B-dependent synthesis of antiapoptotic factors, has been evaluated in a number of published and ongoing trials for solid and hematological malignancies (39). Moreover, it has been reported that the IKK $\beta$  inhibitor MLN120B inhibits TNF $\alpha$ -induced NF- $\kappa$ B activation, resulting in inhibition of the growth of multiple myeloma cell lines (40). We showed that a newly developed NF- $\kappa$ B inhibitor, dehydroxymethylepoxyquinomicin (DHMEQ), can be utilized for controlling allograft rejection (41). A recent study has shown that a potent and selective inhibitor of Nedd8-activating enzyme, MLN4924, disrupts cullin-RING ligase-mediated protein turnover, leading to apoptotic death in human tumor cells by dysregulation of S-phase DNA synthesis (42). Furthermore, treatment of diffuse large B-cell lymphoma cells with MLN4924 results in rapid accumulation of phosphorylated I $\kappa$ B $\alpha$ , decrease in nuclear p65 content, reduction of NF- $\kappa$ B transcriptional activity, and G<sub>1</sub> arrest, ultimately resulting in apoptosis induction. Therefore, detailed research using MLN4924 may clarify the function of TRIM40 in regulation of the NF- $\kappa$ B pathway. In conclusion, further functional analysis of TRIM40 may provide therapeutic benefits not only for inhibition of the growth of gastrointestinal cancers but also for the prevention of chronic inflammatory bowel diseases.

### Funding

Grant-in-Aid for Scientific Research (21390087) from the Ministry of Education, Culture, Sports, Science and Technology of Japan; Ono Cancer Research Fund.

### Acknowledgements

The authors thank Toshio Kitamura for the plasmids, Tomoki Chiba for the antibodies, Sinya Tanaka and Takashi Saku for the cell line and Yuri Soida for help in preparing the manuscript.

*Conflict of Interest Statement:* None declared.

### References

- 1 Reymond, A. *et al.* (2001) The tripartite motif family identifies cell compartments. *EMBO J.*, **20**, 2140–2151.
- 2 Urano, T. *et al.* (2002) Efp targets 14-3-3 sigma for proteolysis and promotes breast tumour growth. *Nature*, **417**, 871–875.

- 3 Gack, M.U. *et al.* (2007) TRIM25 RING-finger E3 ubiquitin ligase is essential for RIG-I-mediated antiviral activity. *Nature*, **446**, 916–920.
- 4 Quaderi, N.A. *et al.* (1997) Opitz G/BBB syndrome, a defect of midline development, is due to mutations in a new RING finger gene on Xp22. *Nat. Genet.*, **17**, 285–291.
- 5 Avela, K. *et al.* (2000) Gene encoding a new RING-B-box-Coiled-coil protein is mutated in mulibrey nanism. *Nat. Genet.*, **25**, 298–301.
- 6 Miyajima, N. *et al.* (2008) TRIM68 regulates ligand-dependent transcription of androgen receptor in prostate cancer cells. *Cancer Res.*, **68**, 3486–3494.
- 7 Kano, S. *et al.* (2008) Tripartite motif protein 32 facilitates cell growth and migration via degradation of Abl-interactor 2. *Cancer Res.*, **68**, 5572–5580.
- 8 Kikuchi, M. *et al.* (2009) TRIM24 mediates ligand-dependent activation of androgen receptor and is repressed by a bromodomain-containing protein, BRD7, in prostate cancer cells. *Biochim. Biophys. Acta*, **1793**, 1828–1836.
- 9 Kamitani, T. *et al.* (1997) Characterization of NEDD8, a developmentally down-regulated ubiquitin-like protein. *J. Biol. Chem.*, **272**, 28557–28562.
- 10 Lammer, D. *et al.* (1998) Modification of yeast Cdc53p by the ubiquitin-related protein rub1p affects function of the SCFCdc4 complex. *Genes Dev.*, **12**, 914–926.
- 11 Liakopoulos, D. *et al.* (1998) A novel protein modification pathway related to the ubiquitin system. *EMBO J.*, **17**, 2208–2214.
- 12 Read, M.A. *et al.* (2000) Nedd8 modification of cul-1 activates SCF(beta-TCP)-dependent ubiquitination of I $\kappa$ B $\alpha$ . *Mol. Cell Biol.*, **20**, 2326–2333.
- 13 Wu, K. *et al.* (2000) Conjugation of Nedd8 to CUL1 enhances the ability of the ROC1-CUL1 complex to promote ubiquitin polymerization. *J. Biol. Chem.*, **275**, 32317–32324.
- 14 Xirodimas, D.P. *et al.* (2004) Mdm2-mediated NEDD8 conjugation of p53 inhibits its transcriptional activity. *Cell*, **118**, 83–97.
- 15 Watson, I.R. *et al.* (2006) Mdm2-mediated NEDD8 modification of TAp73 regulates its transactivation function. *J. Biol. Chem.*, **281**, 34096–34103.
- 16 Abida, W.M. *et al.* (2007) FBXO11 promotes the Neddylation of p53 and inhibits its transcriptional activity. *J. Biol. Chem.*, **282**, 1797–1804.
- 17 Oved, S. *et al.* (2006) Conjugation to Nedd8 instigates ubiquitylation and down-regulation of activated receptor tyrosine kinases. *J. Biol. Chem.*, **281**, 21640–21651.
- 18 Stickle, N.H. *et al.* (2004) pVHL modification by NEDD8 is required for fibronectin matrix assembly and suppression of tumor development. *Mol. Cell Biol.*, **24**, 3251–3261.
- 19 Xirodimas, D.P. *et al.* (2008) Ribosomal proteins are targets for the NEDD8 pathway. *EMBO Rep.*, **9**, 280–286.
- 20 Gao, F. *et al.* (2006) Neddylation of a breast cancer-associated protein recruits a class III histone deacetylase that represses NF $\kappa$ B-dependent transcription. *Nat. Cell Biol.*, **8**, 1171–1177.
- 21 Karin, M. *et al.* (2002) NF- $\kappa$ B in cancer: from innocent bystander to major culprit. *Nat. Rev. Cancer*, **2**, 301–310.
- 22 Ghosh, S. *et al.* (1990) Activation *in vitro* of NF- $\kappa$ B by phosphorylation of its inhibitor I $\kappa$ B. *Nature*, **344**, 678–682.
- 23 Mercurio, F. *et al.* (1997) IKK-1 and IKK-2: cytokine-activated I $\kappa$ B kinases essential for NF- $\kappa$ B activation. *Science*, **278**, 860–866.
- 24 Yaron, A. *et al.* (1998) Identification of the receptor component of the I $\kappa$ B $\alpha$ -ubiquitin ligase. *Nature*, **396**, 590–594.
- 25 Hatakeyama, S. *et al.* (1999) Ubiquitin-dependent degradation of I $\kappa$ B $\alpha$  is mediated by a ubiquitin ligase Skp1/Cul1/F-box protein FWD1. *Proc. Natl Acad. Sci. USA*, **96**, 3859–3863.
- 26 Mantovani, A. *et al.* (2008) Cancer and inflammation: a complex relationship. *Cancer Lett.*, **267**, 180–181.
- 27 Hu, Y. *et al.* (1999) Abnormal morphogenesis but intact IKK activation in mice lacking the IKK $\alpha$  subunit of I $\kappa$ B kinase. *Science*, **284**, 316–320.
- 28 Pikarsky, E. *et al.* (2004) NF- $\kappa$ B functions as a tumour promoter in inflammation-associated cancer. *Nature*, **431**, 461–466.
- 29 Karin, M. *et al.* (2005) NF- $\kappa$ B: linking inflammation and immunity to cancer development and progression. *Nat. Rev. Immunol.*, **5**, 749–759.
- 30 Li, Q. *et al.* (2005) Inflammation-associated cancer: NF- $\kappa$ B is the lynchpin. *Trends Immunol.*, **26**, 318–325.
- 31 Okumura, F. *et al.* (2010) TRIM8 modulates STAT3 activity through negative regulation of PIAS3. *J. Cell Sci.*, **123**, 2238–2245.
- 32 Hayden, M.S. *et al.* (2004) Signaling to NF- $\kappa$ B. *Genes Dev.*, **18**, 2195–2224.
- 33 Wu, C.J. *et al.* (2006) Sensing of Lys 63-linked polyubiquitination by NEMO is a key event in NF- $\kappa$ B activation. *Nat. Cell Biol.*, **8**, 398–406.